DEVELOPMENT OF A NOVEL INSERT TO INCREASE SERVICE LIFE AND PERFORMANCE OF BOLTED CONNECTIONS

By

Bryon J. Hall

A THESIS

Submitted to
Michigan State University
in partial fulfillment of the requirements
for the degree of

MASTER OF SCIENCE

Mechanical Engineering

2011

ABSTRACT

DEVELOPMENT OF A NOVEL INSERT TO INCREASE SERVICE LIFE AND PERFORMANCE OF BOLTED CONNECTIONS

By

Bryon J. Hall

As composite materials take on a more prominent role in ground vehicles, there is an increasing need to find efficient methods of joining composites to dissimilar materials; one of the most common methods is to use a mechanical fastener within a thin metallic sleeve. Studies have shown this method can decrease the strains in the vicinity of the bolted connection. This study explores the use of new, novel insert in joining composite to dissimilar materials. Instead of using a metallic insert, a standard 12.70 mm hex bolt is modified to allow a liquid to be injected into the joint through the bolt. Once the material has hardened, it creates a sleeve around the bolt, similar to the metallic insert. In this study, single-lap joints were fabricated using the novel insert. These materials were tested both quasi-statically and using ballistic-strain rates. The results were recorded using Digital Image Correlation as well as several qualitative methods. The results show the novel insert is preferable over a non-reinforced joint and does provide some benefits compared to a metallic insert.

TABLE OF CONTENTS

LIST OF FIGURES

INTRODUCTION

The purpose of this research is to investigate one possible method of increasing the failure load of a single-lap bolted joint, specifically by adding an insert to the joint. For the purposes of this paper, a single-lap bolted joint is a joint in which two materials are overlapped and are joined together using a mechanical fastener. The mechanical fastener consists of a bolt, two washers, and a nut consists of a bolt, two washers, and a nut; the washers are placed between the head of the bolt and the composite panel and between the nut and the metallic panel. Figure 0.1 shows a sectional view of the single-lap shear joint.

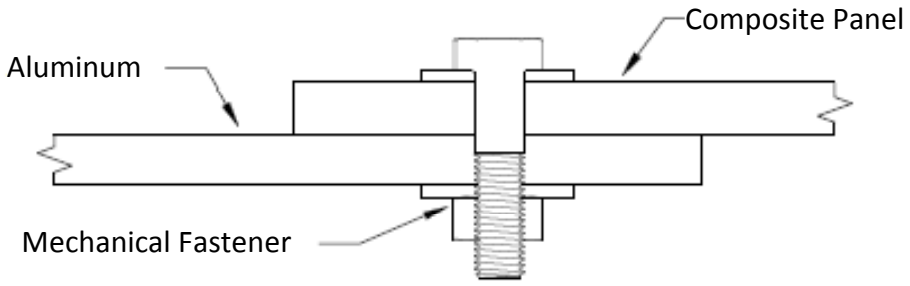

Figure 0.1 – Schematic view of a single-lap bolted joint

An insert is any material which is inserted into the joint and acts as a boundary between the bolt and the outer diameter of the bolt. Prior researched has focused on machined inserts; machined inserts are thin bushing, usually metallic in nature, inserted into the joint prior to securing the panels by means of a mechanical fastener. A machined insert is fabricated so as to be flush with the outer diameter of the bolt hole. The inside diameter is designed for minimal clearance between the bolt and the machines insert. Machined inserts are typically designed using hard materials such as aluminum or steel, although softer materials such as epoxies,

nylons, or other plastics can also be used. Figure 0.2 shows an exploded view of a single-lap shear joint with a machined insert.

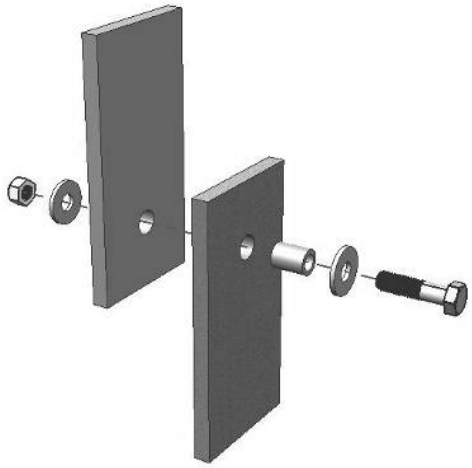

Figure 0.2 – Exploded view of single-lap bolted joint with machined insert

The intent of this research is to focus on the development of the novel, or injected, insert. The insert is formed by injecting a liquid into a fastened single-lap bolted joint using a standard grade 8 hex bolt that has been modified by machining channels into the bolt. After the liquid has cured it will form a soft insert around the bolt. Figure 0.3 shows a schematic view of a single-lap bolted joint with an injected insert.

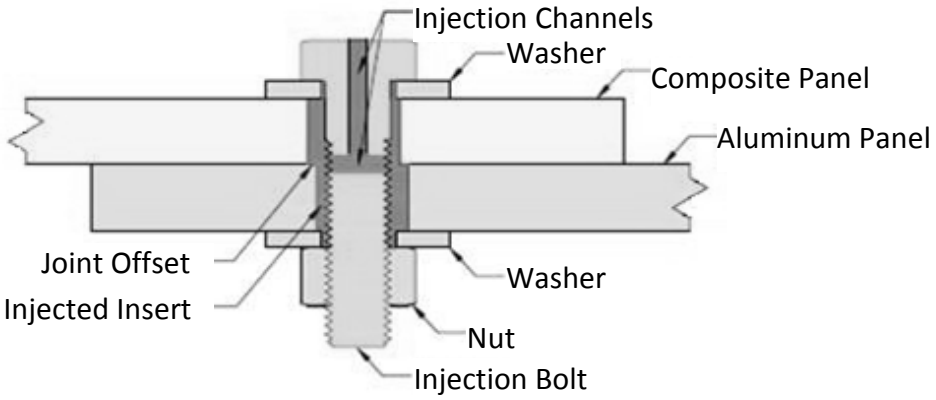

Figure 0.3 – Schematic view of a single-lap bolted joint with an injected insert

Purpose

The injected insert has several possible over a machined insert. A machined insert must be machined to specifically match both the size and the geometry of the hole. Even machined inserts intended for use on similar diameter or shape holes must be carefully machined to ensure a tight fit between the insert and the inside diameter of the hole. Furthermore, a machined insert requires the bolt hole to be aligned in every panel. An injected insert is dependent only on the size of the bolt used in joining the objects. Once the size of the fastener has been determined, an injected insert would be able to conform to a variety of hole sizes and geometries. Additionally, as shown in Figure 0.3, an injected insert is able to accommodate an offset within the bolt hole.

Metallic inserts can be susceptible to environmental factors. In addition to the clearance between the bolt and the inside diameter of the machined insert, if any defects exist between the outside diameter of the insert and the hole, a liquid or fine particle such as sand could become entrapped within the joint, causing long-term damage. An injected insert would seal the joint, preventing water or other liquids from becoming entrapped in the fastening system.

A machined insert can be susceptible to long term fatigue or vibration caused by poor clearances between the bolt and the insert or between the insert and the outer diameter of the hole. Additionally, if the joint is subjected to vibration, the nut could loosen, resulting in failure of the joint. An injected insert conforms to the hole geometry and results in a tight fit preventing damage caused by clearance within the fastening system. Additionally, an injected insert creates a seal within the fastening system and can be designed to create a locking

mechanism between the nut and the bolt, reducing the possibility of prolonged vibration loosening the bolt and causing failure.

Three possible disadvantages of using the injected insert have been identified and will be investigated. The removal of material from the bolt to create the injection channels could weaken the bolt and change the failure mode of the composite. The locking mechanism noted earlier could make removal of the bolt from the joint more difficult, decreasing the reparability of the joint. The material properties of a self-curing liquid, specifically the elastic modulus and the shear modulus, will typically be lower than for a machined insert. This could result in a less efficient distribution of strain.

Chapter 1 – Novel Insert Bolt Design

Chapter 1 will focus on the development of the bolt design for the injected insert. This chapter will investigate different channel designs and how each channel design affects the quality of the cured injected insert. This chapter will investigate different methods which can be used to inject the liquid into the joint; it will consider the advantages and disadvantages several different means of injection. The chapter will also introduce the standard testing procedure which will be used throughout the research.

Previous Research

Investigation into the addition of an adhesively bonded metallic insert to a composite bolted joint was conducted by Nillsson [1]. In his study, a FE analysis was performed using a 2-D FE analysis with a width-diameter ratio of 4.0 and edge-diameter ratio of 2.5. A hole diameter of 10 mm was chosen for the composite only model and a diameter of 14 mm, with a insert wall thickness of 2 mm for the bonded insert models. It was determined high compressive and tensile forces existed respectively at 0 and 90 degrees from the direction of loading. The addition of an aluminum and steel insert resulted in a stress concentration reduction of 40% and 55%, respectively; experimental verification was performed using a $(90/0/90/0/-45_2/+45_2/90/0/-45/45)_S$ 3.6mm laminate of similar dimensions loaded in dual shear using a finger-tight bolt. These results showed an increase in failure of load of 30% and 55% while using bonded steel and aluminum inserts, respectively. Unbonded inserts reduced the failure load 10% to 20%, respectively, from the bonded inserts.

Herrera-Franco and Cloud [2] performed similar studies regarding strain relief inserts. In their study, they used R1500/1581 3.55 mm thick laminate with an edge-diameter ratio >3, width-

diameter ratio >8, and hole diameter of 6.35 mm. They loaded the panel in double-shear without inserts and using soft (photoelastic cement) and hard inserts (aluminum) with a 3.18 mm wall thickness. Using moiré fringe patterns, the results showed a significant reduction in stress at an angle 0 degrees from the axis of loading. Figure 1.1 shows strains parallel to the load axis for various types of machined inserts and Figure 1.2 shows the strain perpendicular to the load axis for various types of machined inserts.

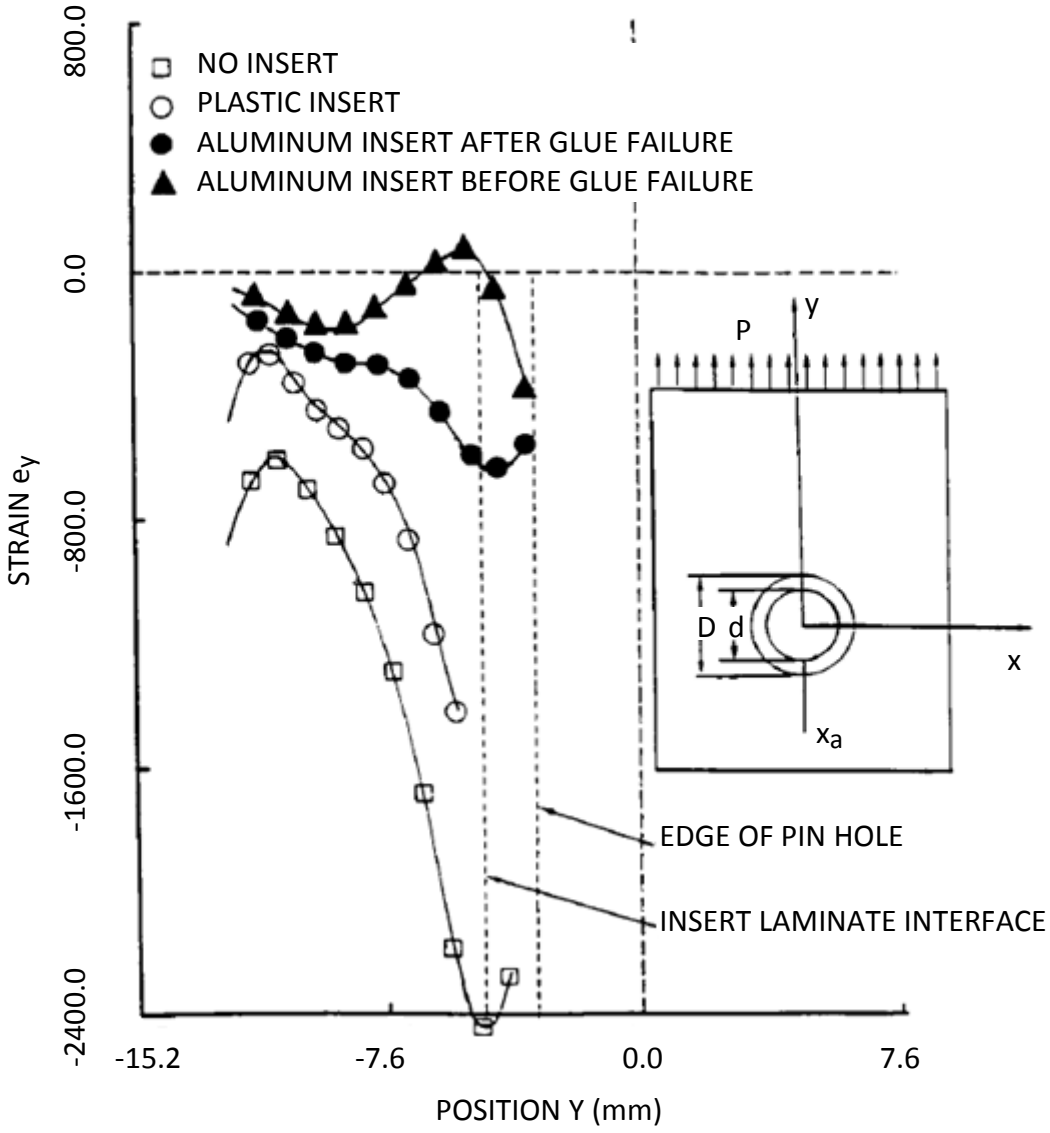

Figure 1.1 – Strain parallel to load axis for some machined inserts. [2]

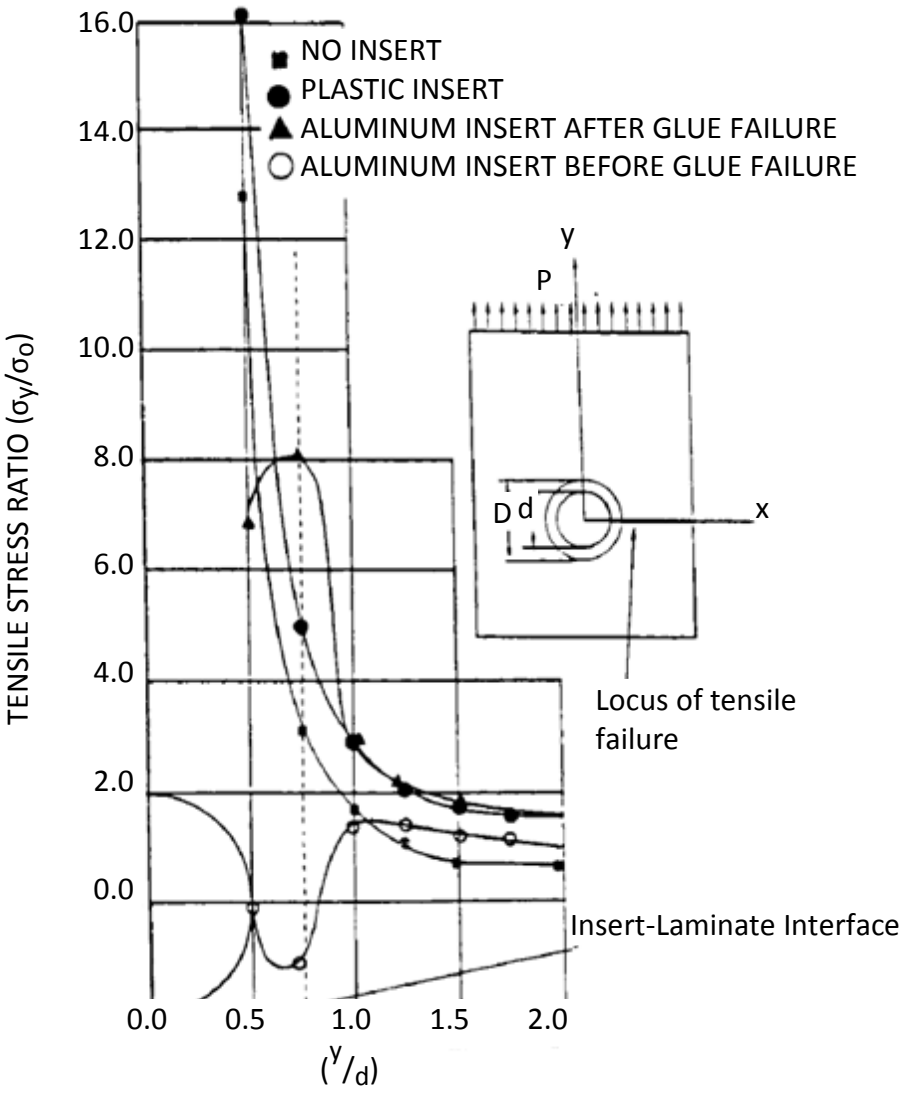

Figure 1.2 – Strain perpendicular to load axis for some machined inserts. [2]

Camanho et.al [3] conducted research into the addition of bonded metallic inserts to both single-shear bolted joints as well as double-sheer bolted joins. Their research concluded that although bonded metallic inserts reduce the stress concentrations in both types of joints, double-shear bolted joints did not experience an increase in failure load. Furthermore, they showed aluminum inserts are preferable to steel inserts because of lower developed tensile stresses. Based on this research, using thin composite panels they investigated the effects of

using a tapered insert that protrudes from the joint. They tested three types of inserts: type "A", type "B", and type "C". A type "A" is shown in Figure 1.3. A type "B" is similar to type "A" except the edges of the insert are not tapered. A type "C" insert is a traditional insert which does not protrude from the joint. They found that, due to increased load transfer surfaces, a Type "A" insert resulted in a 27% and 282% increase in failure load opposed to a Type "B" and Type "C" insert, respectively.

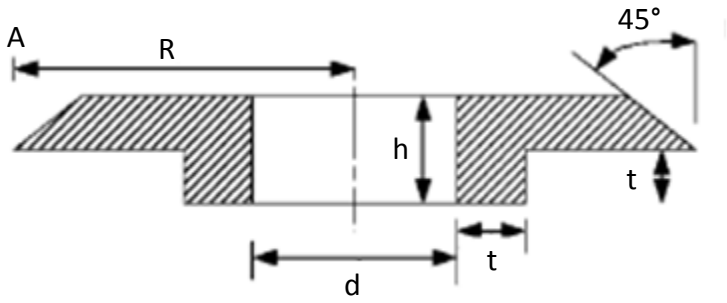

Figure 1.3 – Insert geometry for reinforcing thin composite plates. [3]

Herrington and Sabbaghian [4] investigated the effect of radial clearance on the failure strength of thin composites. Using thin composites loaded in double-shear, they examined the failure loads using washer to bolt-diameter ratios between 1.124 and 1.005. Their results showed a significant correlation between high ratios and low ratios. A low ratio significantly increased the failure load whereas, and despite high clamping loads, a high ratio resulted in a failure load approaching that of a pin-loaded joint. There results concluded the increase in failure load due of a pre-clamping force is due to both the increased frictional load on the plate as well as the ability of a washer to prevent out-of-plane "brooming".

Riccio and Marciano [5] investigated the effects of material and geometrical features on the failure load of bolted composite joints. Using a composite plate 4.16mm thick loaded in single shear, they compared the effects of hole diameter, type of bolt (countersunk vs. protruding),

and joint type (composite-composite vs. composite-aluminum) against the failure load of each combination. Based on their experiments, they concluded that although bolt type does not affect failure load, protruding bolts withstand higher loads prior to damage whereas countersunk bolts experience greater displacement prior to failure. They also found that whereas aluminum-composite interfaces have lower failure loads than composite-composite interfaces, composite-aluminum interfaces result in a more uniform distribution of damage within the composite plate.

Erikkson [6] investigated the effects of lateral constraints, ply orientation, hole diameter and thickness and loading direction on the bearing strength of laminated composited. They used brittle graphite-epoxy T300/914C and toughened graphite-epoxy HTA7/6376 available from Ciba-Geigy. The results were consistent for each composite type and were as follows. Lateral constraints increase the strength because of load transfer through friction forces. Without a constraint, the damage will occur at the bolt-composite interface; with a constraint, the damage will occur at the outer diameter of the constraint. Ploy orientation has little effect on the strength if the majority of the plies are oriented at 0-degree or + 45-degrees. Increasing the hole diameter or increasing the thickness of the composite were found to slightly increase the bearing strength. The loading direction (tension or compression) was found to have little effect on the bearing strength of the composite joint.

Mold Design

Before testing any injection bolt design in an actual single-lap bolted joint it was necessary to determine the effectiveness of the injection bolt design. An effective injection bolt design should result in an injected insert that conforms fully to the geometry of the hold

and is free of any significant defects such as air entrapped within the insert. The optimal injection bolt design should also require the removal of minimal material from the bolt.

This test required the design of a mold that allow for qualitative observation of the injected insert without affecting the insert itself. If a standard single-lap bolted joint were used, the process needed to remove the fastening assembly, which includes the bolt, washers, nut, and injected insert, would require the removal of the nut and washer and would likely result in damage to the injected insert. A break-away mold that would replicate the conditions of the single-lap bolted joint and allow for removal of the bolt assembly without causing damage was designed for this experiment. Note: typically all dimensions were performed using the English system of measurement. However, for consistency only the SI values are shown

Each mold consisted of a square 76.20 mm in length; this length allowed for easy handling and reduced the amount of excess material. A hole 19.05 mm in diameter was drilled through the center of each square. This diameter lessened the tolerances necessary when centering the injection bolt within the hole and created an injected insert equivalent to a machined insert with a 3.18 mm wall thickness.

Each square was cut down through the center of one edge. This cut allowed for the removal of the bolt assembly without causing damage to the injection insert. This split also eliminated the need to removal any part of the bolt assembly. Transparent tape was placed on the exposed edges resulting from the split. The tape acted as a compressible gasket that prevented the liquid from entering the boundary between the adjoining edges of the mold. The tape was also placed on the outer diameter of the bolt hole. This tape resulted in an injected insert that was more transparent than those created without using tape to smooth the

edges of the bolt hole. Figure 1.4 shows one square of a mold with some of the features highlighted.

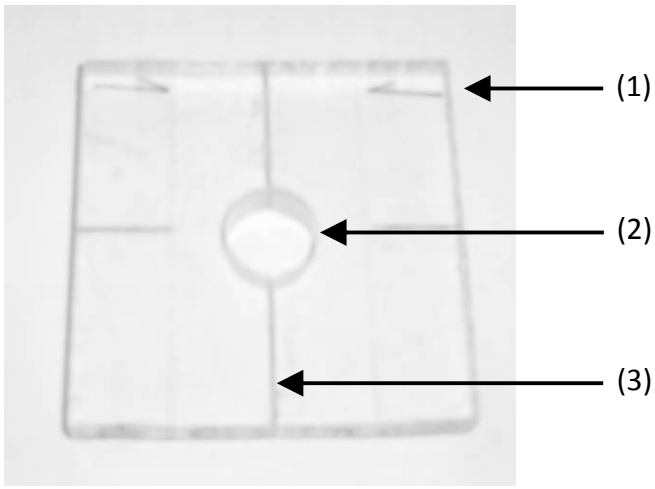

Figure 1.4: Sample Square used for bolt design testing.

The mold consists of two squares, a top half and a bottom half. Each square was 12.7 mm thick and fabricated using the above specifications; this thickness was chosen to mimic the thickness of the composite and aluminum plates used in the actual single-lap bolted joints. The two squares were stacked on each other, with the cut edges aligned parallel to each other. The mold was fabricated using an optically clear high-strength polycarbonate; this provided a cheap lightweight alternative to steel and aluminum and allowed for limited visual observation of the boundary layer between the top and bottom half of the mold. The four pieces of the mold were secured using a commonly available quick-clamp. A completed mold with injection bolt is shown in Figure 1.5.

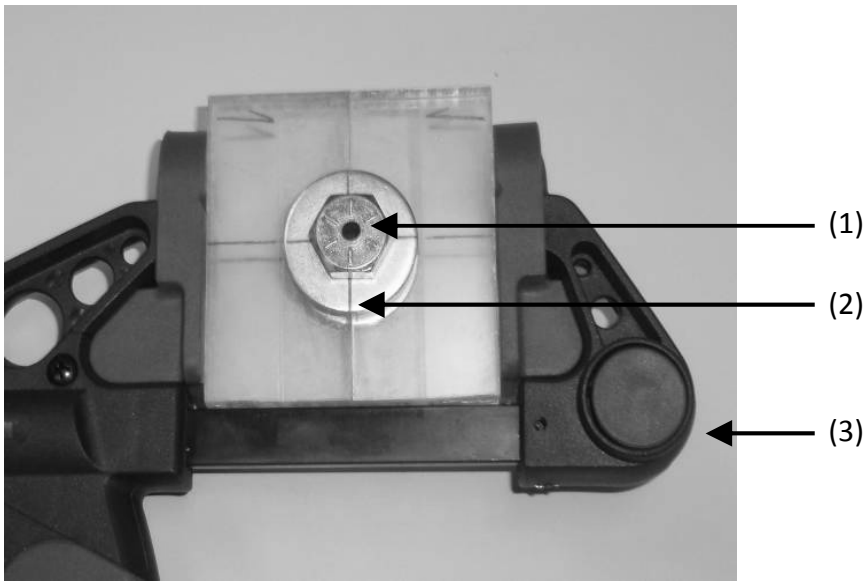

Figure 1.5 – Sample mold assembly with injected insert.

Three important features of the completed mold assembly are shown in Figure 1.5. (1) The material is injected into the bolted through an opening located on the head of the bolt. (2) Centerlines on the mold and the washer allowed the bolt to be nominally centered within the hole providing a uniform insert thickness for the tests. (3) The quick clamp provided a quick method for securing the mold during the curing phase. The 76.2 mm length of the mold was ideal for use with the quick clamp.

Initial Injection Bolt Design

Having developed a mold capable of allowing visual observation of the injected insert without damaging the injected insert or requiring the removal of any portion of the bolt assembly, it was necessary to test the effectiveness of different bolt channel designs. Two different parameters were chosen as variables for the design of the injection bolt; channel diameter and channel quantity. Using the parameters, three different designs were initially developed. The first design uses two thru-channels; thru channels span the entire diameter of the bolt. The

channels are perpendicular to each other and are equally spaced through the 25.4 mm length corresponding to the length of the bolt contained within the bolt hole. The second design contains one thru-channel; centrally located within the 25.4 mm length. The third design contains two half-channels; half channels extend radially from the center of the bolt to the outside of the bolt. The channels are parallel to each other and are equally spaced through the 25.4 mm length. Figure 1.6 shows a schematic view of these three channel designs. The channels of all three designs are 3.18 mm in diameter. The uppermost 6.35 mm of the vertical injection channel was been enlarged to 4.76 mm to accommodate the injection device. Once the liquid been injected into the joint, the injector can be removed from the bolt and a steel rod inserted into the vertical injection channel. This rod serves to replace some of the material removed during fabrication of the injection bolt as well as prevent backflow of the liquid during the curing process.

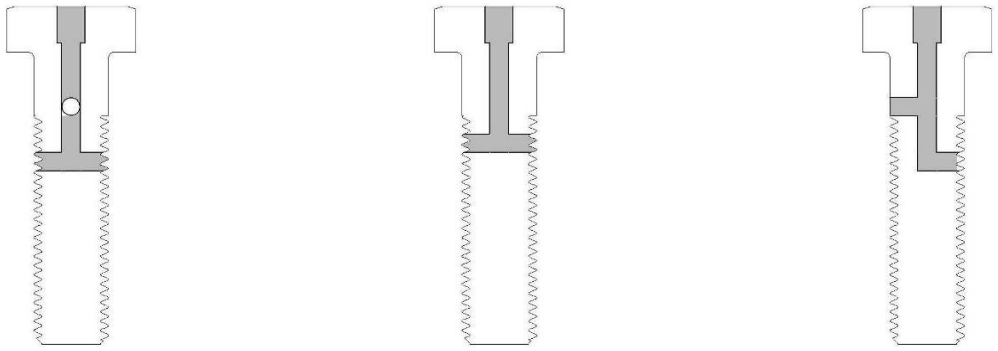

Figure 1.6 – Selected injection bolt designs

Injection Method

Three different methods were considered for the injection method: a human-powered injector, an air-powered injector, and an electrically powered injector. The advantages and

disadvantages of each system were analyzed to determine the most effective injection method for these experiments as well as the best overall method.

The hand powered injector uses disposable syringes with tapered nozzles. The shape of the nozzle allows the syringe to be directly inserted into the injection channel as noted in the injection bolt design dimensions, eliminating the requirement of an intermediary tube. These syringes are available in sizes suitable for the experiments and are readily available at retail stores. However, these syringes have a limited injection pressure and do not have a repeatable method of controlling the injection rate.

The air-powered method uses disposable syringes compatible with shop air, typically 690 kPa. The shape of the nozzle allows the syringe to be inserted directly into the injection channel, eliminating the need of an intermediary connecting tube. These syringes are also available in sizes suitable for these experiments and provide a constant pressure of injection. However, this method requires standard 12VAC power and a supply 690 KPa compressed air. Furthermore, the system requires a significant, onetime expense for initial setup and does not provide an adequate method to prevent excessive spillage of the liquid.

The electrically powered method uses an electrically powered motor to drive the injection of the liquid. As the system relies on a variable-speed battery driven motor, the rate of injection is controllable and the system is portable. However, currently available systems are designed for reservoir volumes of 300 ml or larger. A single injection bolt requires less than 6 ml of liquid. This system also requires a significant onetime expense prior for initial setup.

Based on the advantages and disadvantages of each system above, a disposable 30 ml syringe with a tapered nozzle was chosen as the best option for the experiments conducted for this research. The low cost, ease of use and availability of the components for this system outweighed the lack of control of either the injection rate or the injection pressure. However, if a higher rate of production was required, the electrically powered device would be the best method of the three listed. The reservoir size is suitable for quickly filling multiple injection bolts and the electrically driven motor provides a controlled and repeatable injection rate and pressure. Furthermore, the one-time cost required is diminished as the volume of the production increases.

Injection Bolt Design Qualitative Testing

Tests were performed to validate the mold design and concept of injecting a liquid into a single-lap bolted joint through an injection bolt. Standard grade 8 bolts, 63.5 mm in length with a diameter of 12.7 mm, with varying channel designs and channel diameters of 4.76 mm were fastened in the molds using washers with a 34.93 mm outer diameter and 2.54 mm thickness placed between the mold and nut and between the mold and the bolt head. Epoxy resin was injected into each sample using a disposable 30 ml syringe with tapered nozzle. The injection insert was allowed to cure for 24 hours. After 24 hours, the mold was removed from the quick clamp and visual observations were used to qualitatively estimate each configuration. Figure1.7 and Figure 1.8 show some observations

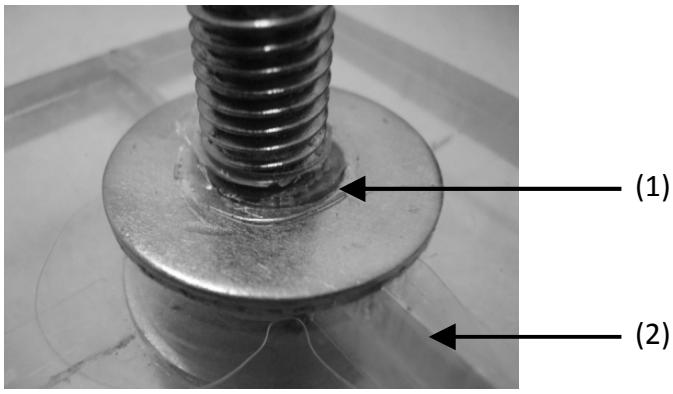

Figure 1.7 – Injection mold after removing nut.

Two important features of the injection mold after removing the nut are highlighted in Figure 1.7. **(1)** Epoxy resin infiltrated the space between the lower washer and the bolt, between the lower washer and nut and (already removed) and between the nut and the bolt. **(2)** Epoxy infiltrated the boundary between the upper and lower halves of the mold. This leakage could be used to create a hybrid adhesive-mechanically fastened joint.

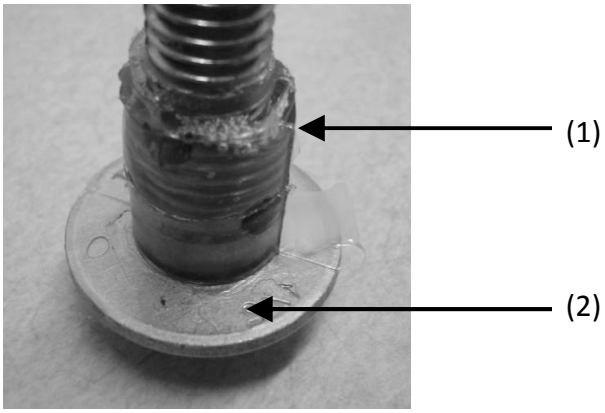

Figure 1.8 – Bolt assembly with lower nut and washer removed.

Two important features of the bolt-insert assembly are highlighted in Figure 1.8. **(1)** Significant air voids were observed near the interface between the insert and the lower washer (already removed). **(2)** Epoxy infiltrated the boundary between the top washer and top half of the mold.

Injection Bolt Design Qualitative Testing Results

The purpose of the qualitative testing was to determine whether an injection bolt could be used to effectively inject a liquid into a single-lap bolted joint and to determine what factors would significantly affect the quality and consistency of the injected insert. Based on these tests, which used a thin epoxy resin with a medium rate hardener, neither the channel design nor the channel diameter had any noticeable effect on the quality and consistency of the injected insert. Every test performed using these two parameters as variables ended with similar results. Every injected insert was of similar quality and consistency. Furthermore, every injected insert had air voids, similar in size and quantity to those shown in Figure 1.8 above, at the location in the injected insert which had the highest elevation as the injected insert was curing.

During the testing a third parameter was observed that did affect the quality and consistency of the insert. During the initial tests, the bolt assembly was hand-tightened, producing a minimal pre-load on the assembly. These samples experiences a significant number of air voids. Additional tests were conducted using bolts that were tightened to 2.82 N-m by means of a torque wrench. These samples had a significantly reduced number of air voids. Figure 1.9 shows a sample tightened to 2.82 N-m.

Figure 1.9 – Bolt assembly and injected insert pre-loaded to 2.82 N-m.

Initial Injection Bolt Design Test and Results

After identifying the parameters that most significantly affected the quality and consistency of the injected insert, it was necessary to determine whether the material removal of the bolt would affect the failure mode of the single-lap bolted joint. Using the results from the validation testing above, a single thru channel bolt, see Figure 1.6 (center figure) with 3.18 mm diameter channels was chosen for the initial testing. The center of the injection channel was in the center of the 25.4 mm length corresponding to the length of the bolt contained within the bolt hole. Two samples were prepared using this injection bolt. One sample used a single-lap bolted joint with an hole diameter of 15.88 mm, corresponding to an insert wall thickness of 1.59 mm. The second sample used a single-lap bolted joint with a hole diameter of 19.05 mm, corresponding to an insert wall thickness of 3.18 mm. Both samples were tested to failure using a controlled displacement rate of 1mm/min to determine the effect of removing material from the injection bolt.

Previous research states that thick composites will fail under net tension and as such these samples were expected to fail by net tension. However, neither sample failed through net tension of the composite. The sample with the3.18 mm wall thickness insert failed by catastrophic shear within the bolt at the plane corresponding to the center of the injection channel. Figure 1.10 shows the failed injection bolt. The sample with the 1.59 mm wall thickness insert was stopped after a brittle failure, presumably in the injected insert, was audibly observed during the test. Upon inspection of the bolt assembly, cracks were observed within the injected insert.

Figure 1.10: Injection bolt failure with 3.18 mm wall thickness insert.

<u>Injection Bolt Design Modifications</u>

Based on the unexpected failure of the sample by shear failure of the bolt, it was necessary to reinvestigate the design of the bolt to improve the strength of the bolt. Upon investigation, three factors were identified which could contribute to increased strain concentrations in the bolt which contributed to the shear failure observed within the injection bolt. (1) A decreased cross-sectional area of the bolt resulting from material removal from the bolt to accommodate

the injection channels. (2) The position of the injection channel was at a location corresponding to the boundary plane between the plates; this plane is also the plane of greatest shear strain within the bolt. (3) The injection channel was positioned at a location in the threaded portion of the bolt. With these observations, a modified design was proposed.

The purpose of the modified injection bolt design was to minimize the effect of the three conditions listed above. The modified injection bolt design accomplishes this goal by the following changes. (1) The modified design uses a single-half channel opposed to a single thru-channel to minimize the material removal from the bolt. (2) The design moves the plane of minimal cross section (the horizontal injection channel) away from the plane corresponding to boundary between the aluminum plate and the composite plate. (3) The design moves the injection channel to an unthreaded portion of the bolt, minimizing the effect of thread strain concentrations on the failure of the bolt. (4) The design reduced the injection channel diameter from 3.18 mm to 2.38 mm. Figure 1.11 shows a schematic view of the modified bolt design compared to the original design. Using the modified design, two additional tests were run using the testing procedure above. Both tests ended by net tension failure within the composite, validating the modified design of the injection bolt.

Figure 1.11: Modified injection bolt schematic (left) compared to original design (right).

Chapter 1 Conclusions

Chapter 1 focused on the initial and design of the injected insert. The novel insert was proposed as a novel method of reinforcing the bolted connection of a composite plate. Opposed to the more traditional method of using a pre-machined metallic insert to reinforce the bolted connection, the novel insert uses a liquid which is injected into the bolted connection by means of a specially designed bolt and is then allowed to cure.

However, before the performance of the injected inserts could be tested under different loading conditions, it was necessary to verify the feasibility of such a design. A bolt had to be created which could be used to inject the liquid into the bolted connection, a method had to be designed which could test the effectiveness of different bolt designs, a method to inject the liquid into the bolt had to be selected, and the bolt had to be tested to ensure the alterations to the bolt would not change the failure mode from composite failure to bolt failure.

The bolt design used a standard 12.70 mm grade 8 bolt; a hole was drilled from the head downward, and channels radiating from this central hole were used to inject the liquid into the bolted connection. Similarly, a break-away mold, which could be removed after the insert had cured, was used to allow evaluation of the quality of the insert. Through testing with multiple channel configurations and diameters, the research showed the design was insensitive to either the channel configuration or the channel diameters. The only factor which noticeably affected the quality of the insert was the preload applied to the bolt before injecting the liquid; higher preloads resulted in cured inserts with fewer air voids than inserts created with lower initial preloads.

Three possible injection methods were identified in this research: human powered, air powered, and electrically powered. The human powered methods proved the most cost effective, being low-cost, disposable, and available in a large variety of reservoir sizes. The most noticeable disadvantage is the lack of pressure which can be applied using a human powered applicator. The air powered method was similar to the hand-powered methods as many of the applicators can be adapted for pneumatic injection; however, this method was not cost-effective as it required a significant one-time cost to purchase the necessary equipment. In regards to a high-volume production, the electrically powered method was the most efficient, having larger capacity reservoirs as well as well as precise control over volume and rate of injection. However, for these experiments this method was also not cost-effective.

Testing of the bolt design in a single-lap bolted connection showed a significant design flaw. The material removal of the bolt, coupled with several strain concentrations factors, caused the bolt to catastrophically fail in shear prior to failure of the composite. A redesign of the bolt, which decreased the channel diameter, moved the injection channel away from the plane corresponding to the boundary between the aluminum plate and the composite plate, and moved the injection channel to the unthreaded portion of the bolt, sufficiently reduced the stress concentrations within the bolt such that the single-lap joint once again failed by net tension of the composite plate.

Chapter 2 – Load-Displacement Results of Inserts

Chapter 2 will focus on the use of load and displacement data to examine the performance of metallic-composite joints mechanically fastened using a single-lap shear joint. This chapter will compare two different types of single-lap shear joints: non-reinforced joints and joints reinforced by means of a machined insert. Due to the limitations of force-displacement measurement, injected inserts were not analyzed using this method. The test will examine the results of joints reinforced with steel and aluminum inserts to those of non-reinforced single-lap joints. The chapter will consider the performance of the inserts at two different wall thicknesses.

Previous Research

Ekh [7] examines the secondary bending caused by attaching carbon fiber and epoxy resin composites to aluminum via a multi-fastener single-lap bolted joint. Ekh seeks to develop a method to measure the bending using a contact-free method. They use a $[\pm 45/0/90]_{4S}$ composite with a ply thickness of 0.13mm The aluminum is 8mm thick and is fabricated from AA7475-T76, and the bolts from titanium. Tensile force is applied to the sample by means of a hydraulic tester. Measurements are obtained using a two-camera system utilizing digital speckle photography. Both cameras were aligned in a plane parallel to the loading direction. When all fasteners were equally tightened, the results showed the primary deflection occurred after the fourth and last fastener. The results also showed the overlap as well as the pre-torque applied to the fasteners will affect both the location and magnitude of the maximum curvature.

McCarthy [8] investigated the load distribution around the fasteners in a multi fastener single-lap shear joint undergoing a tensile load. McCarthy applied the spring model to examine

the load distribution in a multi fastener joint. The spring model is used to account for the clearance of a particular fastener as well as an unequal load distribution. The research uses this method to analyze a $[45/0/-45/90]_{5S}$ using 8 mm titanium bolts as well as steel nuts and washers. The results show that for both single-lap shear joints as well as double-lap shear joints, the results of the spring model reasonably agree with the results of the spring model. Using this agree, a parametric study was conducted which showed that compared to plate thickness and bolt pitch, the clearance of the bolts was the most significant aspect in affect the load distribution of the sample joint.

Khashaba [9] investigated the stress concentrations in the vicinity of a bolted composite joint using both varying washer sized and pre-torques. Khashaba used a $[0/\pm 45/90]_S$ glass fiber composite fabricated by hand lay-up. The specimen was 135mm by 36mm with a 6mm hole drilled 18mm from one end. The experiment considered both the outer diameter of the washer used as well as the pre-torque applied to the bolt before the specimen was tested. The results showed with a constant pre-torque, even though each sample failed at an approximately equal load, the samples with larger washers failed at a greater displacement. When the washer size was held constant and the pre-torque was varied, the results showed the samples with lower pre-torques not only failed at lower loads but also experienced several knees, partial internal failures prior to ultimate failure.

General Testing Procedure

Every test using the application of uniaxial tension was carried out in a similar fashion with minor deviations depending on the type of test performed. Every test was performed on a

Material Testing System 810 (MTS810) with a maximum applicable load of 100kN. The load was applied by a controlled cross-head rate of 1mm/min.

Every test was performed using a single-lap shear joint. Each joint was fabricated using two similarly sized plates joined together using a single 50.80 mm x 12.70 mm bolt with associated nut and washers. Every bolt was a standard grade 8 zinc-plated steel hex bolt with minimum tensile strength of 150 ksi, threaded length of approximately 31.75 mm. Similarly, the nuts were standard grade 8 zinc-plated steel hex nuts with a height of 11.11 mm. The washers were grade 8 zinc-plated high strength steel with inside diameter of 14.30 mm, outside diameter of 34.93 mm, and height between 2.29 mm and 4.57 mm.

Every plate was fabricated using a similar process. Every plate was 203.20 mm in length, 101.60 mm in width, and 12.70 mm in thickness and was oriented vertically. Each plate had two holes drilled 25.40 mm from the bottom of the plate and offset 25.40mm in either direction from the center line of the plate; these holes were used to attach the plates to the testing rig. Each plate had a third hole drilled 50.80 mm from the top edge of the plate located on the center-line of the specimen. This hole diameter, 12.70 mm, 15.88 mm, or 19.05 mm, was determined by the insert wall thickness for the specific test. Figure 2.1 shows the dimensions for an individual plate.

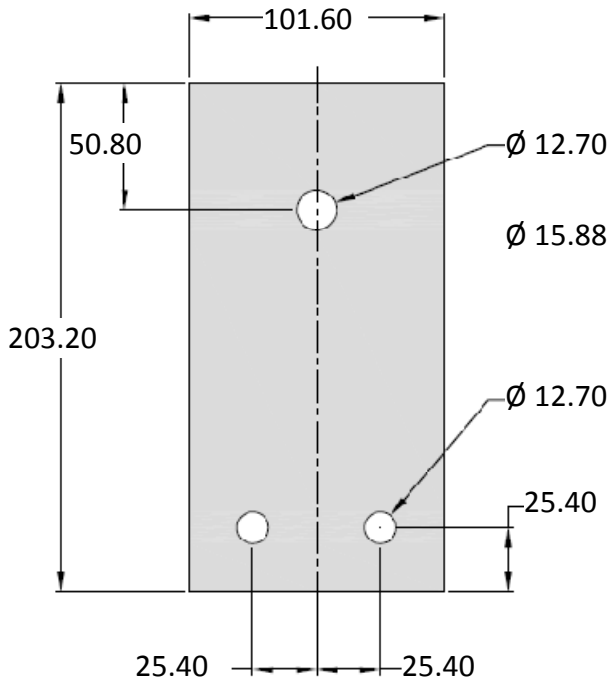

Figure 2.1 – Plate dimensions for single-lap shear joint testing.

Every single-lap shear joint consisted of two plates joined together by means of a mechanical fastener. The front plate, corresponding to the plate closest to the head of the bolt, was fabricated from a 12.70 mm Grade 10 Garolite (glass-epoxy composite) manufactured to military specification MIL-I-24768 with an experimental elastic modulus of 25.6GPa. The back plate was fabricated from a 12.70 mm plate of 7075 aluminum with an elastic modulus of 71.7GPa. The central holes in each plate were aligned with each other and fastened using the above mentioned bolts and accessories. The bolt was secured using a torque of 2.82 N-m and mounted in the uniaxial testing machine using a specially designed fixture which aligned the loading grips with the boundary plane between the two plates. The single-lap shear joint was secured in the mounting fixture by friction gripping and by the two decentralized holes in each plate mentioned above. Figure 2.2 shows a side view of the completed single-lap shear joint

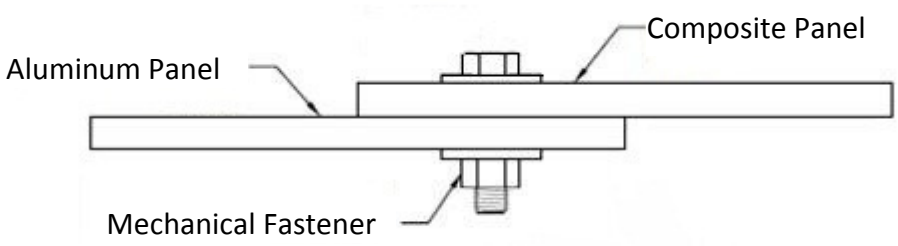

Figure 2.2 – Side view of single-lap shear joint.

The sample was mounted in the uniaxial testing machine using a mount designed to accommodate the single-lap bolted configuration. Figure 2.3 shows the mounting configuration of the single-lap joint within the uniaxial testing machine. Each sample was loaded at a constant cross-head rate of 1 mm/min. The loading was started at 0 N and was continued until the sample failed catastrophically, either by failure within the fastening mechanism or by net tension failure of the composite panel. The load and displacement data was recorded at a rate of 10 points per second.

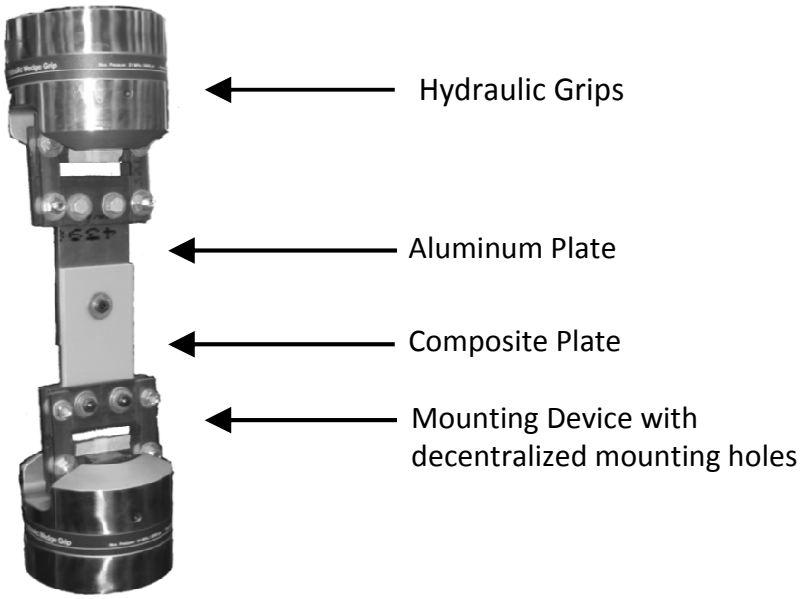

Figure 2.3 – Mounting configuration for single-lap bolted configuration.

Baseline Results

The first set of tests was run using non-reinforced single-lap configuration joints. Four tests were ran using the General Testing Procedure described above. Every sample failed by net tension of the composite plate originating on the boundary between the composite plate and the mechanical fastener at a location approximately 45 degrees from horizontal; Figure 2.4 shows a typical composite plate failure.

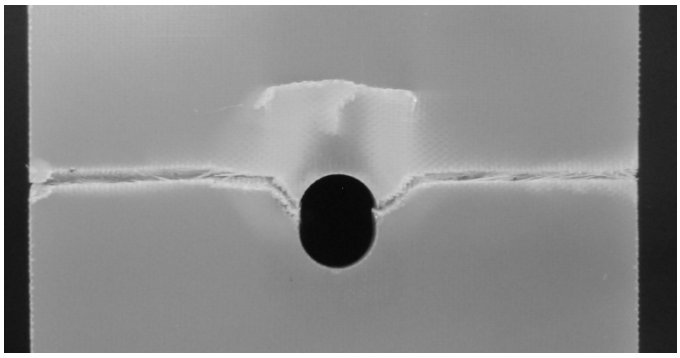

Figure 2.4 – Typical net tension failure of composite plate.

The results were compared against each other to provide a baseline comparison from which the results of the machined inserts could be compared. Figure2.5 shows the load-displacement data for the baseline tests. Examining Figure 2.5 it is apparent the loading mechanism allowed slack to develop within the mounting configuration prior to testing; this resulted in an initial area of non-linear loading prior to the region of elastic loading after the experiment had removed the slack.

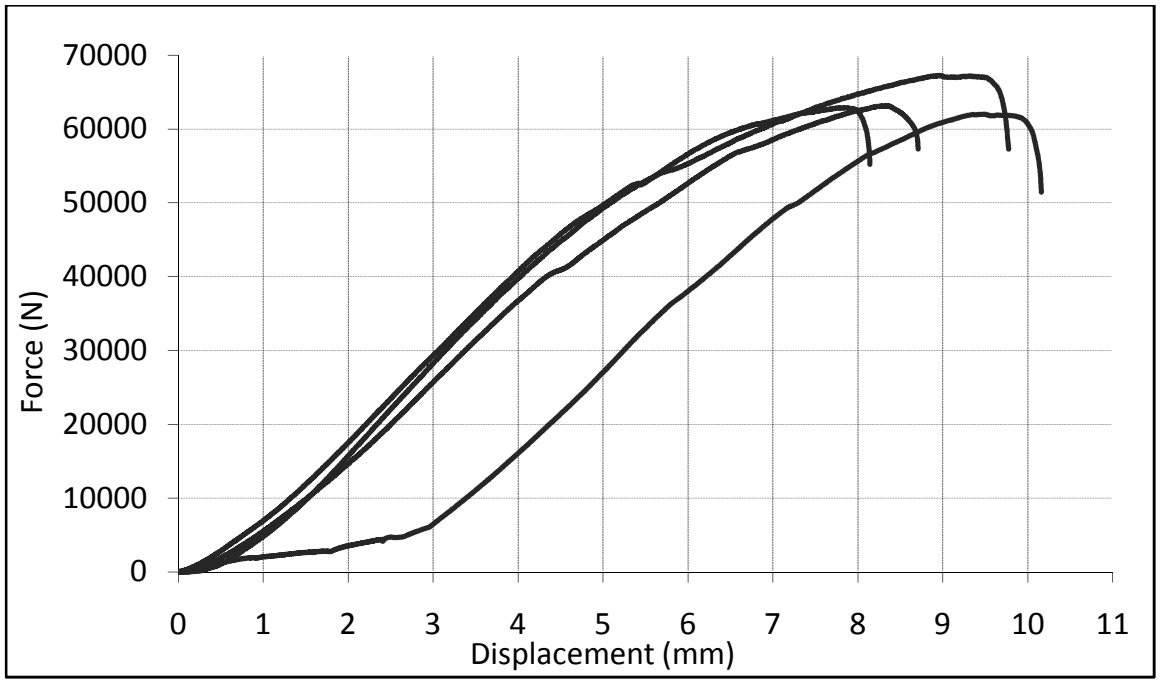

Figure 2.5 – Raw load-displacement data for baseline tests.

To allow for a direct comparison between the data, each data set was normalized to remove the non-linear portion of the data from the results. The normalization process consisted of two steps. During the first step, all data points below 8000 N were removed from the data set. The displacement at this point was then subtracted from the remainder of the data points. This normalization removed the majority of the initial non-linear portion and aligned the resulting elastic loading regions of each data set with each other. Figure 2.6 shows the normalized data for the baseline load-displacement tests and Figure 2.7 shows the failure region of the normalized load-displacement tests.

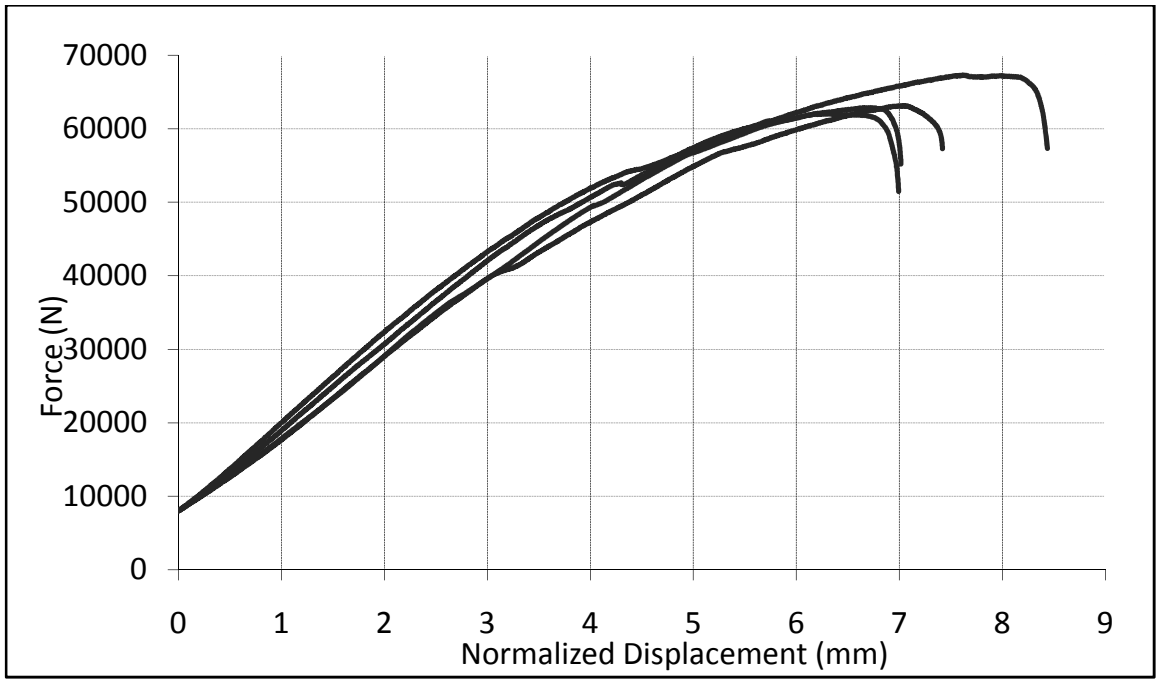

Figure 2.6 – Normalized load-displacement data for baseline tests.

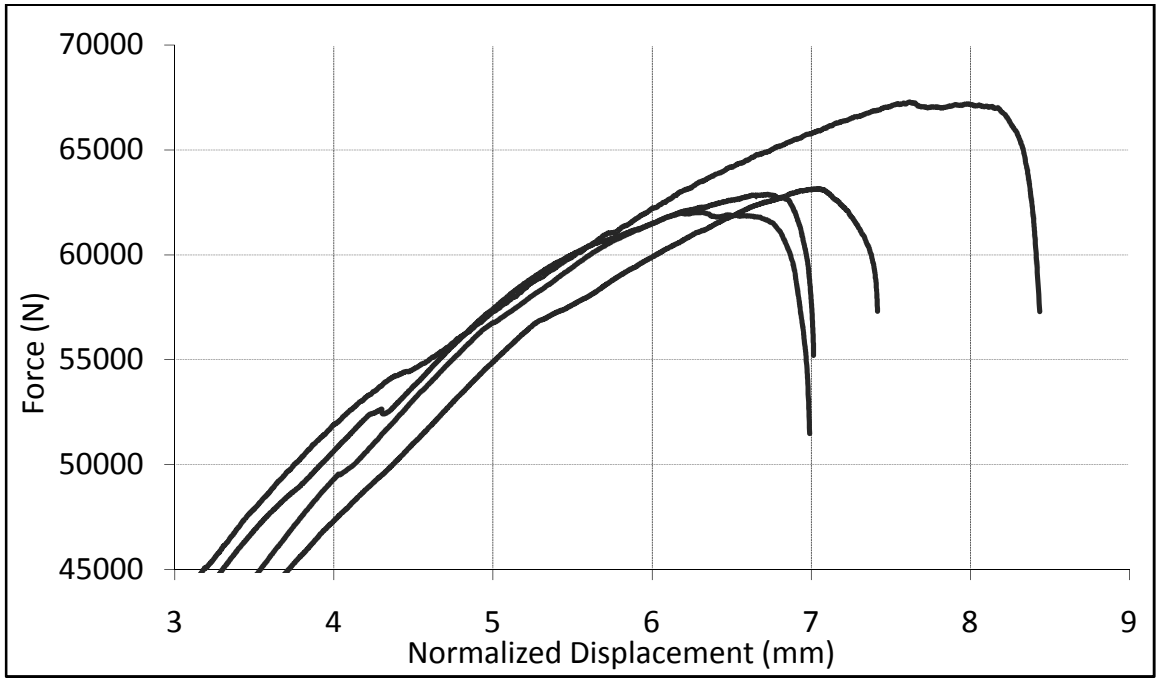

Figure 2.7 – Failure region for normalized data for baseline tests.

Using Figures 2.6 and 2.7, several results can be observed. Using Figure 2.6 it is seen the samples first deviate from the linear loading relationship at approximately. 45 kN. Additionally, each sample has a similar slope, indicating a consistency within the samples. The results also show each sample has little to no bearing failure, indicated by knees in the data, prior to net tension failure. Only one sample, shown in Figure 2.7 at a normalized displacement of 4.3 mm and a load of 53 kN, shows indications of bearing failure. Figure 2.7 also shows, with the outlier exception, that failure occurs at a normalized displacement of 7 to 7.5 mm and a load of approximately 62 kN.

Aluminum Insert Results

The second set of tests was conducted using single-lap configuration joints reinforced using aluminum inserts. Six tests were conducted using the General Testing Procedure described above; three tests used inserts with a 3.18 mm wall thickness insert and three tests used inserts with a 1.59 mm wall thickness insert. Every sample failed by net tension of the composite plate similar to Figure 2.4. The raw data for each test was normalized using the method described in the baseline results. Figure 2.8 shows the normalized load-displacement data for the aluminum inserts and Figure 2.9 shows the failure region for the aluminum insert data. Tests using 3.18 mm inserts are shown by the darker curves and tests using 1.59 mm inserts are shown by the lighter curves.

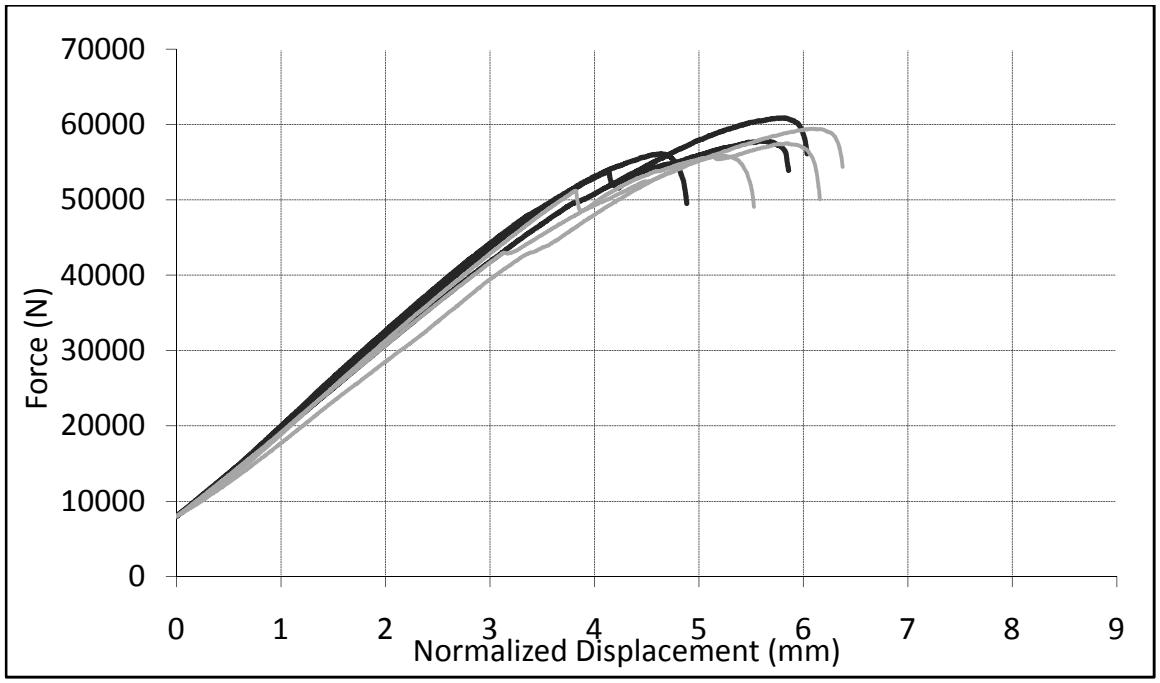

Figure 2.8– Normalized load-displacement data for aluminum inserts.

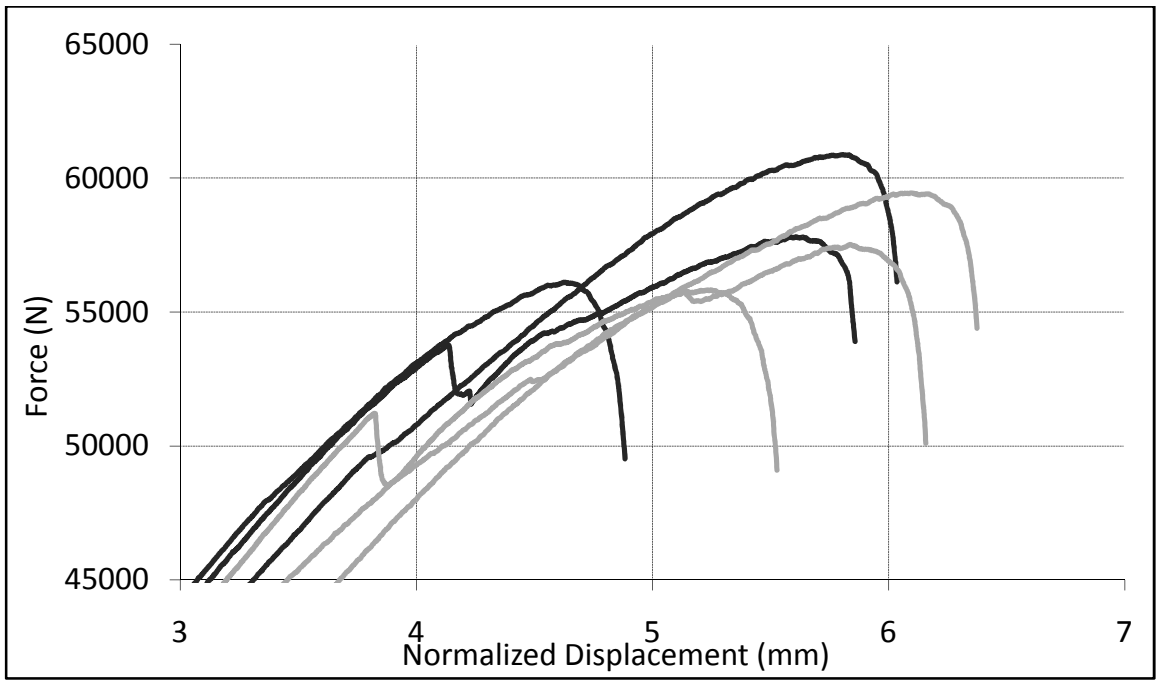

Figure 2.9– Failure region of normalized data for aluminum inserts.

The results shown in Figure 2.8 and 2.9 are similar to the baseline results shown above. Figure 2.8 shows the loading changes from linear to non-linear at approximately 45 kN. Additionally, all six tests exhibited elastic slopes similar to baseline results, indicating an insert does not affect the stiffness of the joint. The greatest difference is shown in Figure 2.9. The average failure load decreased from 62 kN to approximately 55 kN, a difference not entirely by the decrease I cross-sectional area due to the addition of the machined insert. The normalized displacement until failure also decreased from 7 mm to an average of 5.5 mm. Furthermore, several samples experienced showed signs of significant bearing failure to complete net tension failure. However, compared to the baseline results, the aluminum insert results showed considerable variation compared to similar tests. Furthermore, no significant difference was shown between the inserts with a 3.18 mm inserts and the 1.59 mm inserts.

Steel Insert Results

The third set of tests was conducted using single-lap joints reinforced with steel inserts. Six tests were conducted using the General Testing Procedure described above; three tests used 3.18 mm inserts and three tests used 1.59 mm inserts. Every sample failed by net tension of the composite plate similar to Figure 2.4. Figure 2.10 shows the normalized load-displacement data for the steel inserts and Figure 2.11 shows the failure region for the steel inserts data. Tests using 3.18 mm inserts are shown by the darker curves and tests using 1.59 mm inserts are shown by the lighter curves.

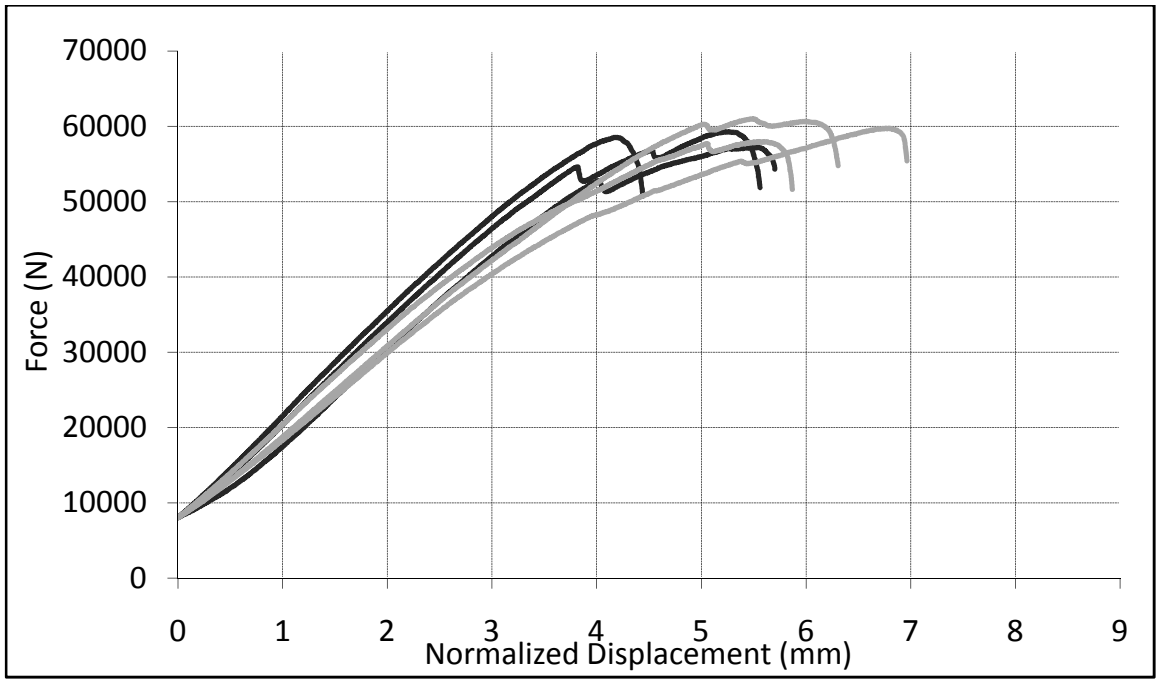

Figure 2.10– Normalized load-displacement data for steel inserts.

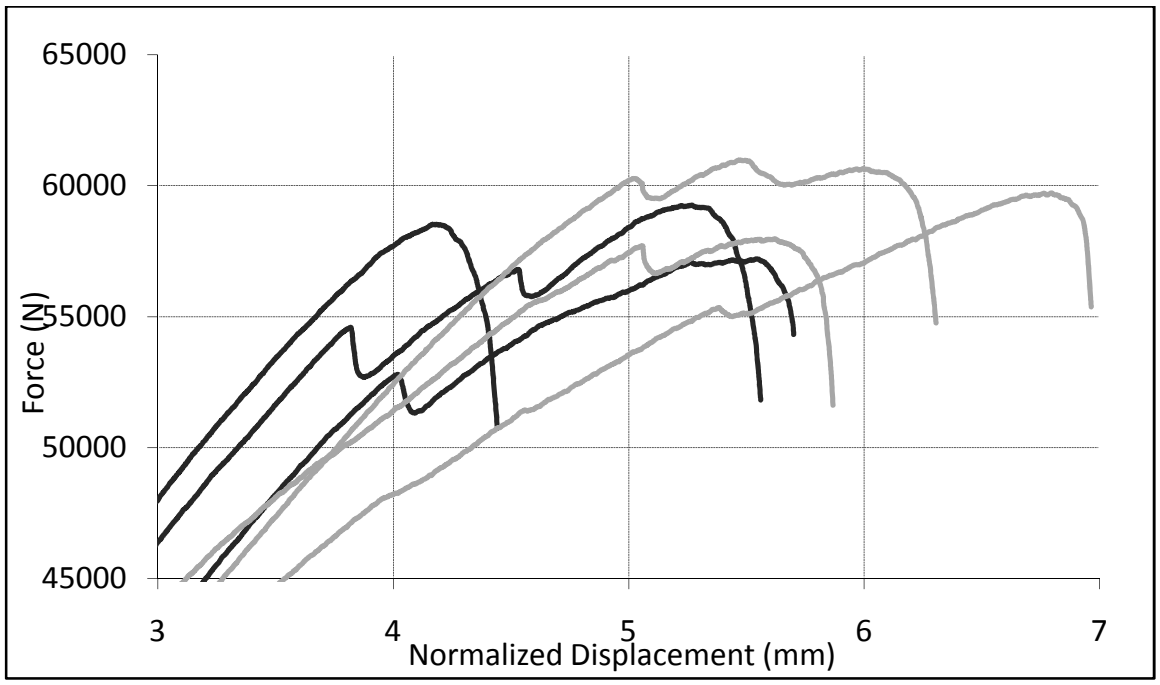

Figure 2.11– Failure region of normalized data for steel insert.

The results shown in Figure 2.10 and 2.11 are similar to the baseline results shown above with a few exceptions. Figure 2.10 shows, similar to the baseline results, the loading changes from linear to non-linear at approximately 45 kN. Additionally, similar to the aluminum results, the stiffness is similar to the baseline results again indicating an insert does not affect the stiffness of the joint. Several differences were also observed. Five of six samples showed signs of bearing failures prior to complete net tension failure. Additionally, the failure load decreased from 62 kN for the baseline to approximately 58 kN, a difference not entirely explained by the decrease in cross-sectional area due to the addition of the machined insert. Differing from the aluminum inserts, the thickness of the insert did appear to affect the failure of the joint. Although the insert thickness did not significantly affect the failure load samples using 1.59 mm inserts failed at a normalized displacement of 6.25 mm whereas samples using with 3.18 mm inserts failed at a normalized displacement of 5 mm.

Chapter 2 Conclusions

The results of Chapter 1 showed that the concept of a novel insert was indeed feasible; it was possible to inject a liquid into a single-lap bolted joint through a bolt without changing the overall failure mode of the joint. The next step was to examine the behavior of both non-reinforced single-lap joints and single-lap joints reinforced different types of inserts. Force-displacement was chosen for the initial analysis because of the simplicity of the test in addition to the range of the test; zero load to failure. However, because of the device used to mount the samples, the results an initial non-linear region resulting from slack within the mounting device. As such, it was necessary to normalize the results to allow for comparison between each test.

The results of the test yielded several results. The baseline tests recorded the highest load to failure as well as the greatest normalized displacement to failure of the three sets of tests. The baseline tests also showed the fewest signs of bearing failure, or 'kneeing' of the three sets of tests conducted. The results also showed the addition of an insert had minimal impact upon the stiffness of the composite plate; however, the addition of an insert tended to cause partial bearing failure prior to complete net tension failure.

The results of the machined inserts were equally useful. The failure load for aluminum inserts decreased from 62 kN for the baseline results to approximately 55 kN. The normalized strain to failure also decreased from 7 mm to 5.5 mm. There wall thickness did not appear significant. The steel inserts showed similar results. The load to failure decreased to 58 kN and the normalized strain to failure decreased to 6.25 mm for the 1.59 mm inserts and 5 mm for the 3.18 mm inserts. The wall thickness did appear to affect the normalized displacement to failure but not the load to failure.

However, the above results are otherwise of limited use. The variation within the each set of tests and the use of load and displacement make it difficult to provide a baseline to which to compare injected inserts. Furthermore, the nature of the net tension failure, as shown in Figure 2.4, indicate the strain fields within the samples are more complex than can be adequately descreibed by load-displacement measurements. It was determined a full-field measurement technique, such as digital image correlation, would be necessary to adequately analyze the performance of a single-lap bolted joint undergoing uniaxial tension loading condition.

Chapter 3 – Digital Image Correlation Results of Inserts

Chapter3 will focus on the use of Digital Image Correlation (DIC) to examine the strain field resulting from applying a tensile loading to the single-lap bolted joints with mechanical fasteners that have not been reinforced with any type of insert (baseline tests). This chapter will compare the results of the baseline tests to tests performed on single-lap bolted joints with mechanical fasteners reinforced with machined inserts as well as joints reinforced with the injected insert. The chapter considers both the effect of material properties as well as the inserts wall thickness.

Digital Image Correlation Introduction

Some common methods of strain measurement systems such as resistance strain gages or fiber-optic strain gages, only measure the average strain that is experienced over the length of the strain gage. With specimens of simple geometry or simple loading conditions, such as a plate in uniaxial tension or pure bending, the use of strain gages is adequate because the strain field is relatively simple and well understood. However, when using a single-lap bolted joint fastening a cross-ply composite laminate to an aluminum plate, the strain field is much more complicated and is less understood. In this situation, the use of a full-field measurement technique such as DIC has many advantages.

DIC is a non-contact optical measurement method used to measure the full-field strain distribution of an object. In DIC, the desired surface is speckled with a random dot pattern, often by using spray-paint. As the object is loaded, images are captured using a digital camera and transferred to a computer. An algorithm is then used to correlate the displacement of each speckle subset relative to the position indicated by a reference image; once the displacements

are known, the strains can be calculated through the use of elasticity equations. Additionally, if necessary a DIC system can be modified by adding a second camera; this configuration is then capable of measuring out-of-plane displacements.

Digital Image Correlation Configuration

For these experiments, DIC was used to better understand the full-field strains developed in the single-lap bolted joint as a result of the uniaxial tension loading configuration. The DIC setup utilized a single Allied Vision Technologies Stingray Progressive CCD camera with a 1624 x 1234 pixel resolution utilizing a bayer mask; a bayer mask is a color filter which increases the sensitivity to green light by using a pattern with 50% green, 25% blue, and 25% red filters. The specimen was illuminated by a single directed light source containing 16 green light emitting diodes (LED) as well as ambient lighting consisting of hi-bay fluorescent fixtures. The samples were mounted in the MTS810 testing apparatus and the load applied according to the specifications established in the general testing procedure. Deviating from the general testing procedure, each sample was only loaded from 0 kN to 30 kN. The loading was paused at every 5 kN (i.e. 5 kN, 10 kN, etc) to acquire the correlation images. Additionally, load and displacement data was not recorded during these tests. The images were transmitted to a personal computer and processed using the Istra 4d software, version 4.2.2.15, to determine the full-field normal strains for both the horizontal axis (X Axis) and the vertical axis (Y Axis). The area of each image showing the bolt assembly was masked (excluded) to remove the reporting of false strains resulting from a non-continuous strain field.

Baseline Results

DIC was used to better understand the in-plane strain fields developed as a result of the uniaxial loading on the single-lap shear joint. DIC was also used to understand what effect, if any, the addition of an insert, either machined or injected, has on the full field strain distribution of the single-lap shear joint. Three sets of experiments were performed to investigate this effect. The first set of experiments examined a non-reinforced joint. The second set of experiments examined the results of samples reinforced with machined inserts. The third set of experiments examined the results of samples reinforced with different types of injected inserts.

The first set of experiments was performed on non-reinforced single-lap shear joints. These results serve two purposes. The first is to provide a comparison between empirical results and DIC. The second is to provide a baseline for the composite joint. The normal strains for the X axis and the Y axis are shown in Figure A1.1 and Figure A1.2, respectively. As the bolt is pushed into the composite because of the loading, it would begin to cleave the composite, (push the material aside), at this point of contact creating a tensile strain in the normal X- axis. This strain is observed in Figure A1.1.

The load is applied to the sample in the negative Y direction (downward) and is transferred to the aluminum plate through the bolted connection; this condition is expected to create a compressive strain in the Y-direction immediately above the bolt hole. From previous testing, ultimate failure of the composite is expected to initiate at the boundary between the composite and the bolted connection at an angle approximately 45 degrees from horizontal. The test configuration utilizes a single-lap shear joint; this configuration creates a bending

moment on the sample, resulting in a compressive strain in the lower portion (the portion below the centerline of the bolt) of the sample. All three of these phenomena are observable Figure A1.2.

Machined Insert Results

A second series baseline tests were performed on preformed inserts. The purpose of this set of experiments was to determine whether similar research performed on thin composite plates could be applied to thick composite plates; this set of experiments also provided a secondary baseline from which to compare the performance of the injected inserts. These tests used 1144 steel and 7075 aluminum inserts with an inner diameter of 12.70 mm and wall thicknesses of 1.59 mm and 3.18 mm.

Figure A1.3 and Figure A1.4 show the x-axis and y-axis normal strains for samples using 3.18 mm aluminum 7075 insert. Based on the results of Figure A1.3 and Figure A1.4 samples using 3.18 mm wall thickness inserts show significant improvement over the baseline results; the insert reduces the y-axis compressive normal strain located above the bolt hole.. Similarly, the insert reduces the cleaving effect seen above the bolt in the x-axis normal strains. In general, the 3.18 mm inserts most effectively reduced the strain gradients.

Figure A1.5 and Figure A1.6 show the x-axis and y-axis normal strains for samples using a 3.18 mm 1144 steel inserts. Comparing these results of the 3.18 mm 7075 aluminum insert, the 1144 steel inserts behaved in a similar manner to the of 3.18 mm aluminum inserts. Both inserts have similar strain profiles for both normal strains and both inserts reduced the strains seen in the baseline results.

The second set of tests was performed using machined considered inserts with a 1.59 mm wall thickness. Figure A1.7 and Figure A1.8 show the x-axis and y-axis normal strains for samples using 1.59 mm 7075 aluminum insert. These results showed that even though these inserts had higher strain magnitudes than the 3.18 mm inserts, the strain profiles are similar to the 3.18 mm 7075 aluminum inserts, with the exception of a more pronounced compressive strain directly above the bolted joint seen in Figure A1.8. The results from the 1.59 mm 1144 steel inserts are comparable to the aluminum inserts of the same wall thickness. These results are shown in Figure A1.9 and Figure A.1.10.

Injected Inserts

The third set of tests was performed using injected inserts. The injection bolts were machined using the modified bolt design described in Chapter 1. The injection materials consisted of a thin epoxy resin with a medium rate hardener, a two-part polyurethane adhesive and a pre-impregnated film adhesive. After application, each material was allowed to cure for at least 24 hours before testing. Inserts with wall thicknesses of 1.59 mm and wall thicknesses of 3.18 mm were tested.

Figure A1.11 and Figure A1.12 show the x-axis and y-axis normal strains for tests using epoxy resin with 1.59 mm epoxy inserts. As the results for the 3.18 mm epoxy inserts are similar to the 1.59 mm epoxy inserts, only the results of the 1.59 mm epoxy inserts are shown. Comparing the results to the previous results, the results show that away from the bolted connection, the strain fields are similar to the strain fields for the 3.18 mm 7075 aluminum inserts. However, as the strain field approached the bolted connection, the behavior of the strain field was similar to the non-reinforced samples. The compressive strains above the bolt

hole, shown in Figure A1.12 are almost identical to the strains produced in the non-reinforced samples.

The second injected insert material tested was a two-part polyurethane. This material is both ductile and has a low elastic modulus. Figure A1.13 and Figure A1.14 show the x-axis and y-axis normal strains for samples using 3.18 mm polyurethane inserts. Using these results, two distinct observations are noted. The compressive strain above the bolted connection is greater in magnitude than the compressive strain for the non-reinforced samples. However, the cleaving effect appears to be significantly decreased when compared to the non-reinforced samples.

The third injected insert material tested was a film adhesive, similar to a pre-impregnated lamina. This material is considered brittle with an elastic modulus similar to the epoxy resin tested; however, unlike the epoxy resin, it has a reinforcing mesh contained within the matrix material. Figure A1.15 and Figure A1.16 show the x-axis and y-axis normal strains for samples using 3.18 mm film adhesive inserts. Using these results, two observations were noted. Unlike the previous injected insert materials, the film adhesive did decrease the compressive strain above the bolted connection. Additionally, similar to the other injected insert materials tested, the film adhesive did decrease the cleaving effect above the bolted connection. Of the three injected insert materials tested, the results of the film adhesive were most suitable when compared to the results of the machined inserts, specifically the 1.59 mm steel or aluminum inserts.

Strain Profiles

As the three sets of experiments described above were taken at different times with the camera positioned at different distances, comparing the full field strain distributions for each image against the other sets of experiments is relatively difficult. To further the analysis, line profiles were recorded for each set of images. The line profiles were created as to capture certain behavioral aspects of each sample that can then be easily compared with the same behavioral aspects from a different sample.

The first line profile was constructed using the x-axis normal strain at a y-value corresponding to the top of the washer (x-x profile); this profile was recorded to analyze the cleaving effect above the bolted connection. Figure 3.3 shows the legend for all four line profiles. Figure 3.4 shows the x-x profile. These results show the non-reinforced joint has the greatest cleaving effect. The strain increases from -0.25 mm/m away from the bolted connection to a magnitude of 2.4 mm/m directly above the bolted connection for a change in magnitude of 2.25mm/m. The 3.18 steel and aluminum inserts had the smallest change, increasing from -1.2 mm/m to -0.3 mm/m. Similarly, the 1.59 mm steel and aluminum inserts also have similar behaviors. The injected inserts show a similar behavior. The polyurethane inserts appears to have the greatest magnitude change, 2.5 mm/m, followed by the epoxy inserts, 2.0 mm/m with the film adhesive having the least change of 1.75 mm/m. This data supports the concept that stiffer inserts, those with a higher elastic modulus (steel and aluminum), perform better than inserts with a low elastic modulus (resin, two-part polyurethane, film adhesive).

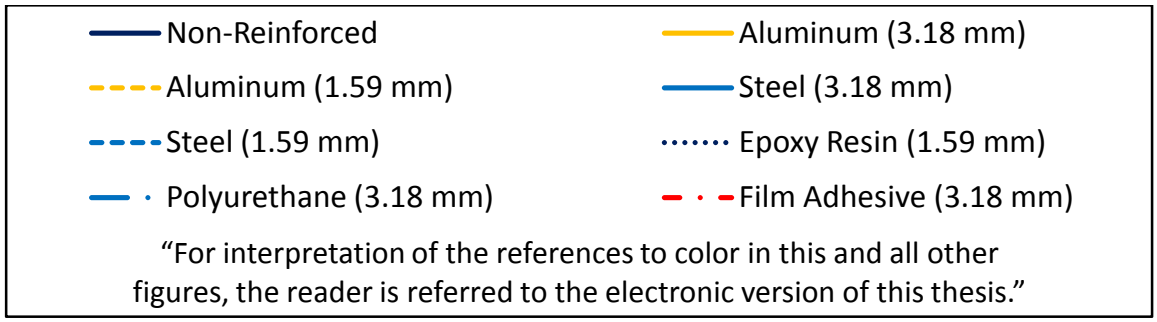

Figure 3.3 – Legend for DIC derived line profiles

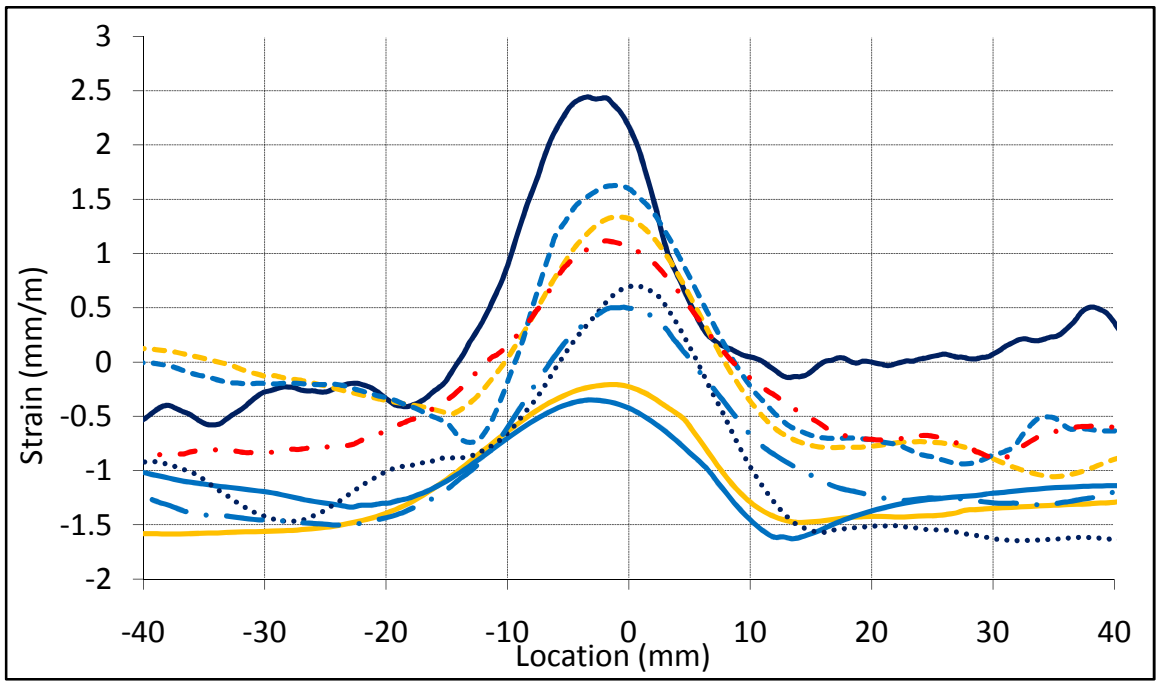

Figure 3.4 – X-X Profile for single-lap bolted connection derived from DIC.

The second profile was constructed using the x-axis normal strain at an x-value corresponding to center of the bolted connection (x-y profile); this profile was recorded to analyze the magnitude between the tensile and compressive strains located above and below the bolted connection, respectively. Figure 3.5 shows the x-y profile. The results of Figure 3.5 show that, in general, the type of insert does not seem to significantly affect the change in magnitude between the tensile strain located above the bolted connection and the compressive strain

located below the bolted connection. Inserts with low tensile strains, the 3.18 mm steel and aluminum inserts, have the highest compressive strain. Similarly, inserts with high tensile strains above the bolted connection, the 1.59 mm steel and aluminum inserts, have a low compressive strain below the bolted connection.

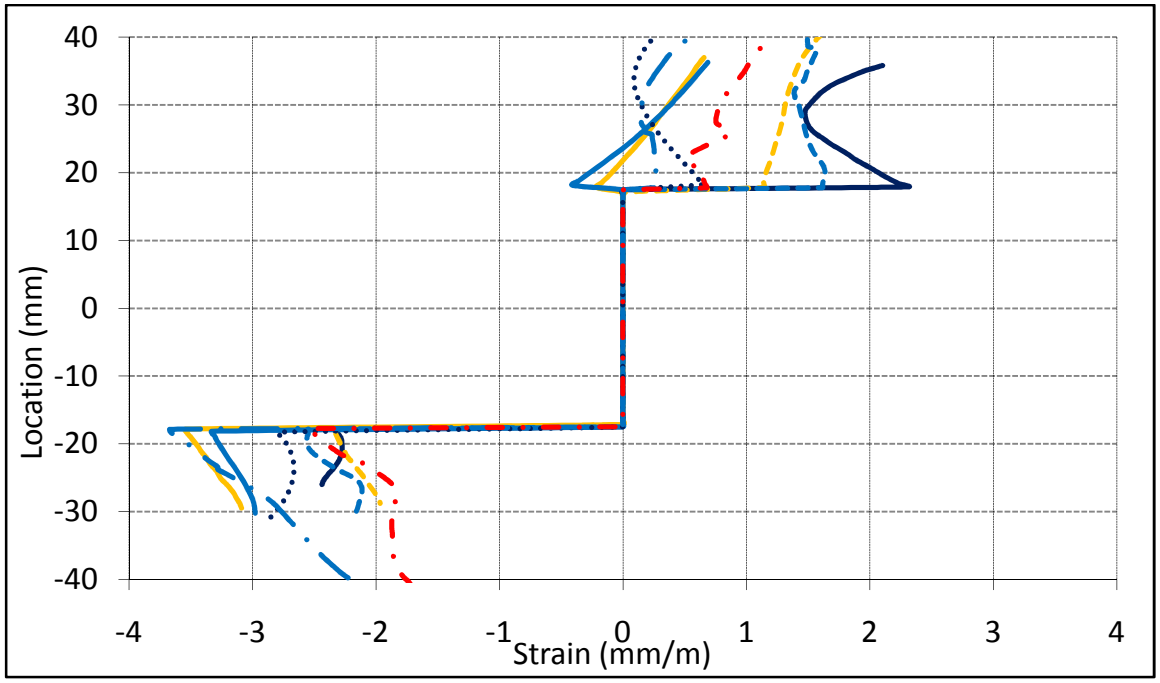

Figure 3.5 – X-Y profile for single-lap bolted connection derived from DIC.

The third profile was constructed using the y-axis normal strain at a y-value corresponding to the top of the washer (y-x profile); this profile was recorded to analyze the compressive strain above the bolted connection. Figure 3.6 shows the y-y profile. The noted results from this profile are similar to those noted for the x-x profiles shown in Figure 3.4. The 3.18 mm steel and aluminum results have similar magnitude changes in strain. Similarly, the material with the lowest elastic modulus has the great change in strain. The most noticeable change is the difference in behavior between the 1.59 mm steel and aluminum inserts. Whereas both inserts show almost identical behavior in the x-x profile (Figure 3.4), in the y-x profile (Figure 3.6), the

steel insert has a significantly increased change in strain compared to the aluminum insert; this data shows that although inserts with higher elastic moduli generally perform better, this performance is also affected by the insert thickness. When using thinner inserts, a more compliant material, such as aluminum, may be more desirable than a less compliant material such as steel.

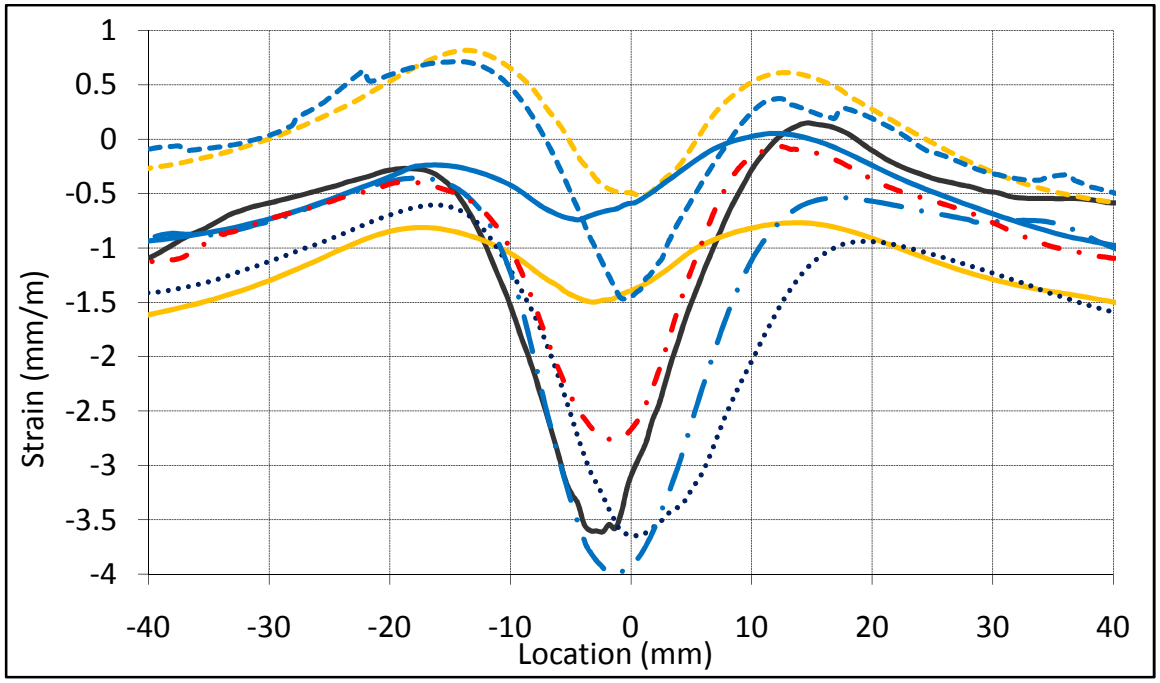

Figure 3.6 – Y-X Profile for single-lap bolted connection derived from DIC.

The forth profile was constructed using the y-axis normal strain at a x-value corresponding to the left of the washer (y-y profile). This profile was recorded to analyze the effect created by the single-lap bolted connection. Figure 3.7 shows the y-y profile. If the plate where under simple tension in the y-axis, it is expected that every point in the plate would experience a tensile strain in the y-axis. However, because of the single-lap configuration, a moment is created about the y-axis that acts to bend the composite plate and cause out-of-plane (z-axis)

displacement. Unfortunately, because the experimental used a one-camera DIC setup, it was not possible to directly measure the out-of-plane displacement. However, as the plate bends, it is expected to most significantly affect the y-axis strains. Therefore, by comparing the y-axis normal strain along a vertical profile, it might be possible to indirectly examine the out-of-plane displacement. The results of the Figure 3.7 show that although the strain for each sample varies, the slope of the strain for every sample in the area of highest interest is approximately equal. Therefore, it might be reasonably concluded that although out-of-plane displacement affects the y-axis normal strain during the tests, as is noted by the unexpected compressive strains shown in the DIC results, the effects of the out-of-plane displacement are similar during each test, indicating it is still valid to compare the results of these experiments to each other, even if it is not possible to extend these results to experiments carried out under other conditions.

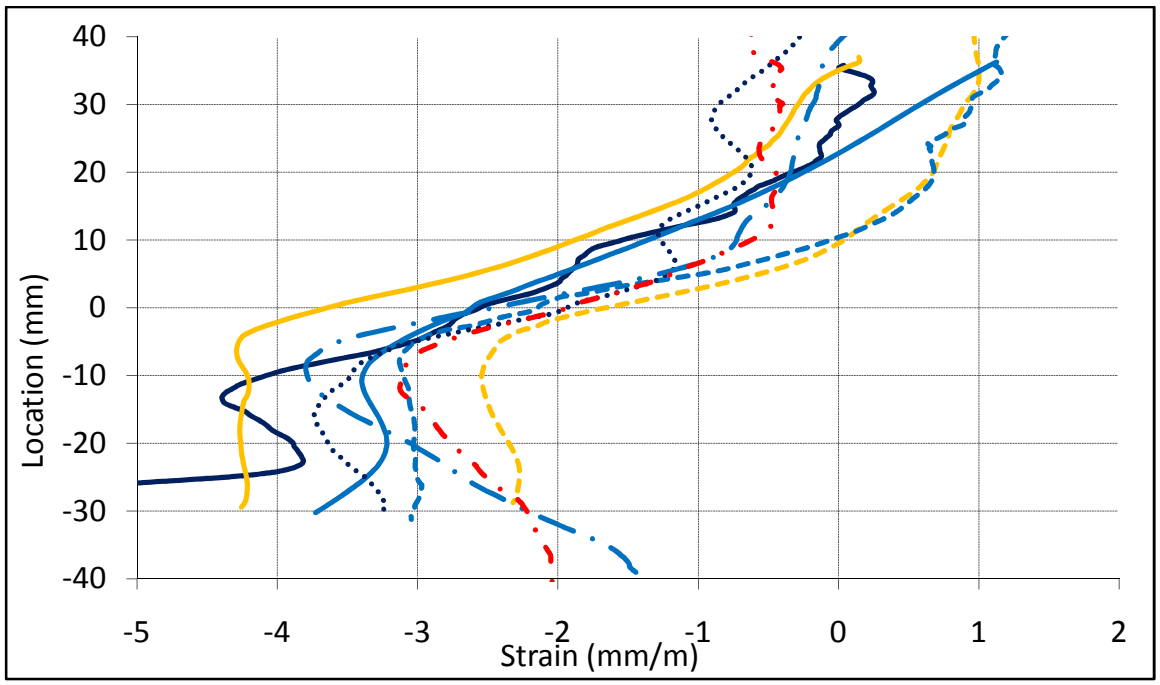

Figure 3.7 – Y-Y profile for single-lap bolted connection derived from DIC.

Chapter 3 Conclusions

As chapter 2 examined, although useful, the use of load-displacement data was insufficient for analyzing the performance of the injected inserts. Scatter within the results and the proximity of the results to each other required the use of a more detailed method to analyze the performance of the inserts. Digital image correlation (DIC) was chosen to analyze the performance of the inserts within the elastic, non-damaging, region of the single-lap bolted configuration.

Three sets of data were acquired using DIC. The first set of data analyzed the results of non-reinforced joints. These results agreed with the visual observations shown in chapter 2. The results of chapter 2 showed failure originated at the boundary of the bolt hole at a location roughly 45 degrees from horizontal. The results of chapter 3 showed this location corresponds with the area of highest normal strain in the vertical direction. The baseline DIC results also showed several other areas of interest: a compressive “contact” stress shown in the vertical normal strain field located above the bolt hole, a “cleaving” tensile strain shown in the horizontal normal strain field located above the bolt hole, and a general compressive strain shown in the vertical normal strain field starting below the mid-point of the bolted connection.

Tests performed on machined inserts as well as some injected inserts reinforced trends seen throughout the previous chapter as well as trends seen in previous research. Stiffer inserts, those with a higher elastic modulus, tended to result in lower “contact” stresses above the bolt hole as well as lower cleaving stress above the bolt hole.

Two other trends were also noticed. Inserts which results in lower cleaving strains tended to have increased compressive strains immediately below the bolt hole whereas inserts with

higher cleaving strains tended to have lower compressive strains immediately the bolt hole. The second trend identified was the un-predicted compressive strain below the midpoint of the bolt was not affected by any insert. The gradient of this strain remained constant for all experiments and the magnitude of the strain appeared independent of the insert material.

The primary disadvantage of this digital image correlation setup was the inability to track out-of-plane displacements. The single-lap bolted configuration by nature produced an out-of-plane displacement within the testing configuration. This bending created an additional stress which was not measureable by the DIC setup utilized. However, as these results were used comparatively and as the out-of-plane bending was predicted to affect each sample equally, it was determined that although the actual numbers reported would be changed by the addition of the bending induced strain , the comparison of the digital image correlation results to each other within these experiments was valid.

Chapter 4 – Performance of Insert Materials under Ballistic Loads

The loading conditions to which these mechanically fastened joints would be exposed to is not best modeled by a low-strain rate environment, as was seen in both Chapter 2 and Chapter 3, it becomes useful to look at the performance of the joints under more severe loading conditions. As such, Chapter 4 seeks to examine the performance of two of the injected inserts, the polyurethane and the film adhesive, under ballistic loading under ballistic loading conditions. As the single-lap bolted joint setup is not practical for this loading condition, an alternative means was developed to test the performance of each of these materials. The delamination, adhesion, and deformation of each sample was considered in the analysis of each sample.

Previous Research

Zaera [10] investigates the effect the adhesive thickness and adhesive properties play on the performance of a ceramic-composite panel undergoing ballistic loading. Zaera researches ceramic-composite armors, specifically, the adhesive layer, as an alternative to monolithic plate armors. These experiments use a 6mm alumina tiles bonded to a 6mm alumina plate with two different types of adhesives: a polyurethane and rubber-toughened epoxy with different thicknesses. The samples were impacted by a 7.62 tungsten carbide AP projectile at 940 m/s. The results showed that both the adhesive type and thickness affected the damage of the sample; thicker layers resulted in less damage to the surrounding tiles but resulted in larger deformations to the aluminum plate as well as increased fragmentation of the ceramic tile. The stiffer adhesive, epoxy, resulted in a lower supporting effect of the aluminum plate.

Lopez-Puente [11] investigated the effect of the thickness of the adhesive layer on the performance of a composite-armor. The experiments used 100x100mm and 51x51mm alumina

tiles arranged in a square enclosed in a 4130 steel frame The samples were bonded to a 2017 aluminum plate using Hysol EA-9361 toughened epoxy resin of carrying thicknesses. The samples were impacted by a 7.62 tungsten carbide round at 940 m/s. After each test, the aluminum plate was removed and cut transversely with a diamond thread. The results showed that the impact caused shear strain in the adhesive and that samples with a thicker adhesive layer better attenuated the shear strain and also better retained portions of the fractured tile. However, samples with thinner adhesive layers experienced less deformation. The optimum thickness was determined to be 0.3mm for all configurations tested.

Panel Design

The tests conducted for both load-displacement and DIC testing used a single-lap bolted configuration; this setup was advantageous because each sample had a simple geometry and simple fabrication method. However, for ballistic loading conditions, this setup is not satisfactory. Under ballistic loading conditions, there is a high probability that upon impact by the projectile, the insert itself as well as the composite plate would be destroyed. The aluminum plate would also be damaged, resulting in an exponential increase of testing costs. As such, a panel design using the desired insert material was used.

The panel design consisted of four basic layers. The back layer used a 0.5” thick aluminum plate; this layer is used to absorb most of the energy from the projectile as well as provide a foundation for the rest of the panel. The second layer consists of the adhesive; the adhesive is used to transmit the shockwave from the front layer to the back layer as well as adhere the front layer to the back layer. The third layer consists of ceramic tiles. The ceramic tiles are used to dull the projectile, if necessary, and absorb some of the impact energy of the

projectile. A small offset is included between each tile and is filled with a rubbery material designed to attenuate the transmission of the shockwave from tile to tile. A forth layer consisting of glass-reinforced composite is also used; however, the purpose of this layer is to contain ceramic spalling as well as prevent bowing of the ceramic tiles. This layer does not serve a significant role in the performance of the panel. Figure 4.1 shows a diagram of a finished panel without the glass reinforced composite overwrap layer.

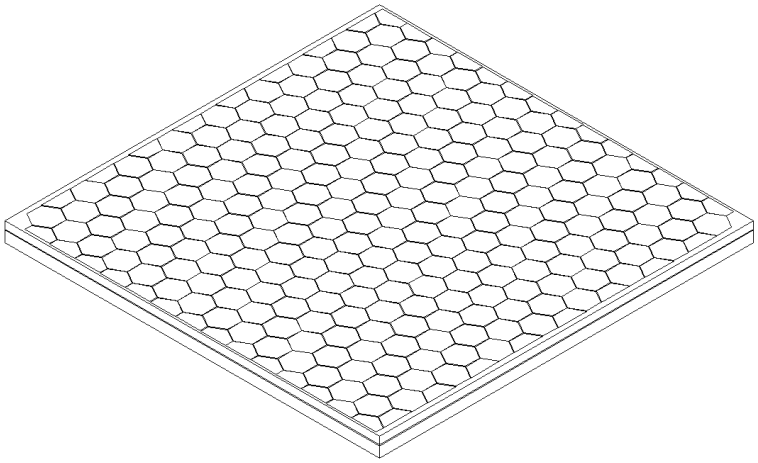

Figure 4.1 – Completed test panel for ballistic loading.

Although this design is not the same as the single-lap bolted configuration used for the earlier experiments as well as several advantages. 1) The purpose of the inserts in the single-lap configuration is to distribute the forces created by the bolt and decrease the localized strains as well as decrease strain gradients. The purpose of the adhesive in the panel design is to distribute the shockwave to the aluminum panel. 2) Similar to the wall thickness of the single-lap configuration, the adhesive thickness of the panel can easily be adjusted to examine the effect of thickness on the performance. 3) The size of the panel can easily be scaled,

allowing for multiple tests to be performed on a single panel with a minimal increase in fabrication time.

Determining Equivalent Thicknesses

The primary advantage of using the above panel design is the ease with which the adhesive thickness can be altered. This is significant because the method used to apply the polyurethane to the panel is fundamentally different than the method used to apply the film adhesive to the panel.

The polyurethane remains a liquid shortly after mixing and retains a constant thickness during the cooling process. As such, the thickness of the adhesive layer in the panel can be controlled by using spacers between the aluminum panel and the layer of ceramic tiles. However, the film adhesive is initially applied to the panel in discrete layers as a solid object. Furthermore, as the film adhesive is cured, a portion of the adhesive will liquefy, causing the thickness to decrease during the cooling process. As previous research has indicated the thickness of the adhesive can significantly affect the performance of the panel, it became necessary to determine a correlation between the initial thickness of the film adhesive before curing and the final thickness of the film adhesive after curing.

In order to establish a correlation between the initial, uncured thickness of the film adhesive to the final, cured thickness of the film adhesive, an experiment was conducted. Four small samples representative of the panel design was fabricated. The back layer of each sample was constructed from an aluminum plate. The adhesive layer of each sample consisted of preselected number of layers of the film adhesive; for this experiment samples were fabricated using three layers, four layers, six layers, and seven layer. The top layer consisted of ceramic

tiles positioned similar to the ceramic tiles on the actual test panels. Figure 4.1 shows a test sample used in this experiment.

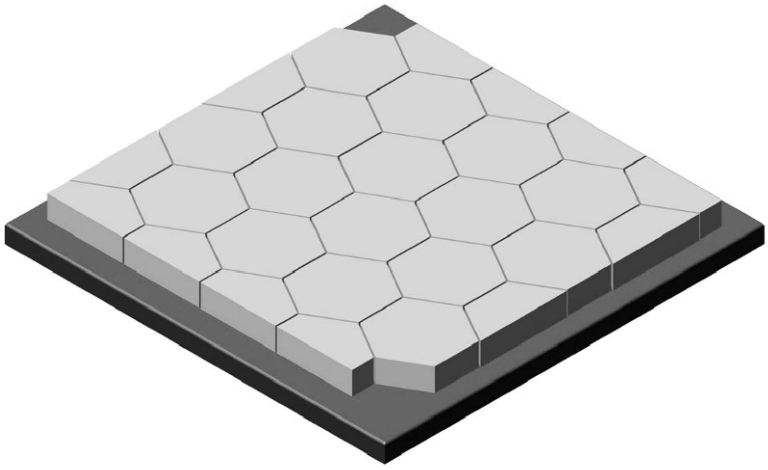

Figure 4.1 – Sample panel for determining equivalent thicknesses.

After each panel had been fabricated, the thickness of the panel was measured and recorded at several points; the average values were normalized and plotted. These values are shown in Figure 4.2 by the diamond markers. The panels were then cured according to the manufacturing recommendations; a weight was placed on each sample to minimize movement of the ceramic tiles during the curing process. After the curing process had completed, the thickness of each sample was measured at several location and the average values were normalized and plotted. These values are shown in Figure 4.2 by the square markers. Using this data, it was determined five layers of the film adhesive corresponds most accurately to the thickness of the adhesive when using the polyurethane.

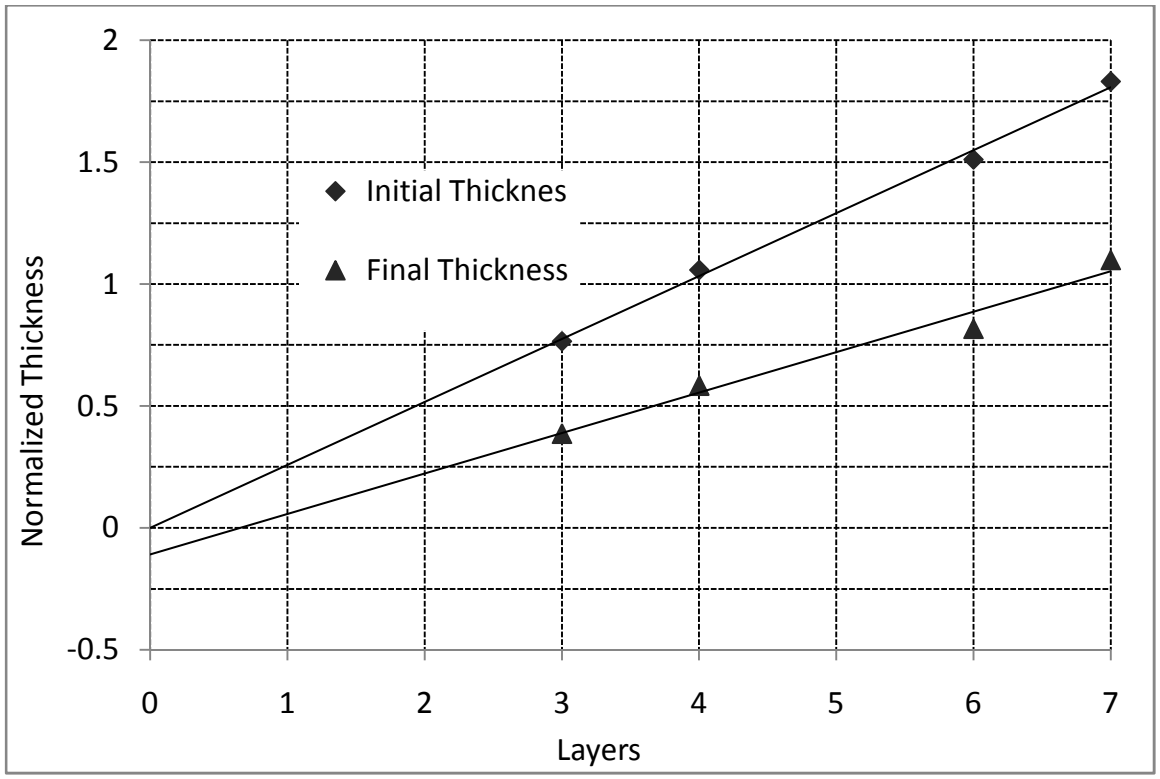

Figure 4.2 – Initial and final thicknesses for film adhesive samples.

Extrapolating the initial thickness values to a theoretical sample with no layers of film adhesive the data correlated precisely to the thickness of the aluminum panel and ceramic tiles. A similar method, when applied to the final thickness data, yielded a slight offset as is shown in Figure 4.2. However, due to movement of the ceramic tiles during the curing process this is considered acceptable error.

Testing Procedure

Based on the results from Figure 4.2 four panels were fabricated for experimental purposes. Two panels were fabricated using the polyurethane using the standard thickness of the adhesive. One panel was created using four (4) layers of the film adhesive. One panel was created using five (5) layers of the film adhesive. The purpose of the experiment was to

qualitatively measure the deformation of the aluminum panel (shape and location), the level of delamination between the aluminum plate and the ceramic tiles, and the adhesion of the fragmented ceramic tiles to the adhesive. However, as no previous research existed to identify how the panels would perform under the ballistic conditions, one panel fabricated using the polyurethane was used as a gauging panel. This panel was tested using several projectiles at different projectiles to determine which combination of projectile/velocity was best suited for the objectives.

Using the results of the gauging panel, it was determined two different tests could be performed on each panel without the results of one experiment affecting the results of the other experiment. The first experiment used a low mass, pointed-edge projectile at a high velocity (Projectile A). The purpose of the experiment was to determine the effectiveness of the adhesive by analyzing the deformation of the aluminum panel at the impact site as well as the retention of the ceramic fragments by the adhesive at the impact site; this experiment was designed not to fully penetrate the sample. The second experiment used a higher mass, blunt-edged projectile at a lower velocity (Projectile D). The purpose of this experiment was to examine the adhesion properties of each material when subjected to a high level of damage. This experiment was designed to cause complete penetration of the sample. The experiment using Projectile A was completed a total of six times per panel; the experiment consisting of Projectile D was tested a total of 3 times per panel

Testing Results

After the panels had been tested, the glass-reinforced composite layer is carefully removed and the panels examined; four aspects of each panel were examined. 1) The

deformation, shape and location, of the aluminum panel caused by the Projectile A tests. 2) The adhesion of the fragments of the ceramic tiles impacted by the projectile during the Projectile A tests. 3) The cumulative level of delamination between the aluminum plate and the ceramic tiles caused by the Projectile A and Projectile D tests. 4) The localized delamination between the aluminum plate and the ceramic tiles caused by the Projectile D impacts. In general, the results showed the panel using the polyurethane adhesive outperformed the panels using the film adhesive as the adhesive layer.

The shape and location of the aluminum deformation for the panel fabricated using polyurethane tended to be more spherical in nature; this shape is indicative of a better distribution of the shockwave as it propagated through the adhesive. The shape and location of the deformation resulting from the panels fabricated using the film adhesive tended to be more parabolic in nature with a greater maximum deformation, as defined by the distance from the plane of the undeformed aluminum to the farthest point of the deformation. Additionally, indications of plugging, or material failure within the aluminum, were also observed in these samples. The shape and location of the deformation indicate a lesser degree of distribution of the shockwave as it propagated through the adhesive. Furthermore, the indications of plugging indicate the material was closer to complete failure.

The sample fabricated using the polyurethane retained more of the ceramic shards resulting from the Projectile A impact. Other than the area immeadiately adjacent to the impact site of the projectile, the majority of the ceramic shards remained adhered to the adhesive. As actual images of the impact area were not available, Figure 4.3 shows a image representative of the fragmented ceramic tile adhesion obtained from previous research.

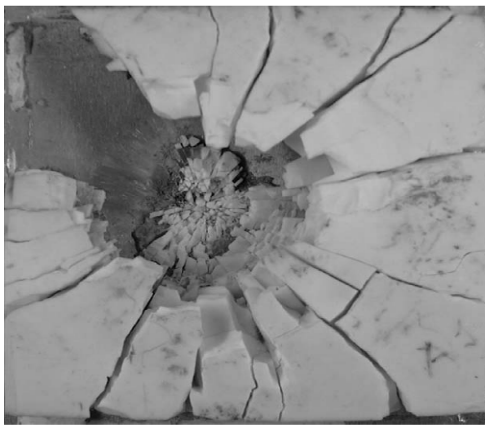

Figure 4.3 – Representative tile adhesion of polyurethane sample from Puente. [11]

The samples fabricated using the film adhesive performed poorly in retaining ceramic shards resulting from the Projectile A impacts. Once the glass-reinforced composite layer had been removed, it was found little to none of the ceramic shards remained adhered to the adhesive. Furthermore, when viewed from the front, a greater level of damage to the aluminum plate was observed when compared to the sample fabricated using the polyurethane adhesive. As an actual image of the impact area was not available, Figure 4.4 shows a representative image of the fragmented tile adhesion of the film adhesive from previous research.

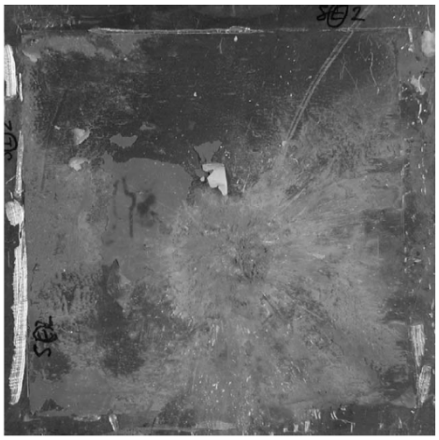

Figure 4.4 - Representative tile adhesion of film adhesive samples from Puente. [11]

The sample fabricated using the polyurethane retained good adhesion during the tests. After the glass-reinforced composite layer was removed, it was observed the ceramic tiles not directly affected by the projectile impacts remained adhered to the aluminum panel. However, for both samples created using the film adhesive, it was observed that complete delamination had occurred between the aluminum panel and the ceramic tiles. However, due to the manufacturing process of the samples, it was not possible to determine whether the delamination was a result of the projectile impacts or whether the delamination occurred during the curing process.

The level of localized delamination resulting from the Projectile B impacts was similar for both the panel fabricated using polyurethane and the samples fabricated using film adhesive. For all tests using Projectile B, the tiles within the area of the aluminum affected by the impact delaminated from the aluminum panel but remained adhered to the adjacent ceramic tiles. Additionally, for all tests, regardless of the adhesive used, the primary damage was limited solely to the tile impacted by the adhesive.

Chapter 4 Conclusions

Although the panel design represents a departure from the single-lap bolted configuration in the previous chapters, the design has the distinct advantage that it provides the opportunity to examine the behavior of the adhesive under more severe the loading conditions of ballistic impacts; a feature which the single-lap bolted configuration does not allow.

One of the primary difficulties encountered with this design is that previous research has shown the overall performance of the panel is highly sensitive to the thickness of the panel;

as the film adhesive is applied in discrete layers and will change in thickness as the adhesive is cured, it was necessary to determine a method to correlate the initial thickness of the film adhesive to the final thickness of the film adhesive. The high degree of correlation and accuracy within the results of the experiment showed a simple linear correlation could be used to determine an equivalent thickness.

Using the results of the previous experiment, three samples were fabricated, one using polyurethane as an adhesive and two using film adhesive, and tested. The results from these tests showed the polyurethane adhesive, which is more ductile and has a lower modulus of elasticity than the film adhesive, performed better in every area of interest. The sample using the polyurethane retained a majority of the ceramic fragments created by the projectile impacts and did not show any signs of delamination during the impact. Inversely, the panels fabricated using the film adhesive retained few if any of the ceramic fragments created by the project impacts and showed signs of complete delamination during the experiment. Additionally, the samples created using the film adhesive proved more difficult to fabricate and, because of the initially solid, discrete nature of the film adhesive, likely contained more flaws within the original construction. Contrary to the previous chapters, which indicate a harder insert with a higher modulus of elasticity is preferable, the results of this chapter indicate a softer material with a lower modulus of elasticity is preferred as those materials have a greater ability to distribute and attenuate shock waves resulting from ballistic impacts.

Summary

Three objectives were considered when conducting this research. These objectives were: to explore the process of mechanically joining dissimilar materials using the concept of a injected insert; asses some of the advantages and disadvantages of using an injected insert; compare the results obtained from samples using injected inserts against similar samples containing more traditional machined inserts. In general, the research was successful in meeting all of these objectives.

Conclusions

Chapter 1 explored the feasibility of mechanically joining dissimilar materials using an injected insert. Preliminary experiments concluded a phase-changing material, such as an epoxy resin, could be injected into the bolted connection through a modified bolt to form an injected insert with sufficient quality. Additional experiments were performed to further optimize the bolt; through these experiments It was determined that neither the channel design or the channel diameter had any significant effect on the consistency of the injected insert. Only the pre-torque applied to the bolt before injecting the material affected the consistency of the bolt. Samples with higher initial pre-torques resulted in samples with a greater consistency in the injected insert. Samples with lower pre-torques exhibited significant air voids within the injected insert.

Chapter 2 and Chapter 3 explored methods of comparing traditional machined inserts against injected inserts. Load-displacement measurements obtained from tension testing experiments provides some results, but were of limited value. The load-displacement results showed that samples without any type of insert generally failed at higher loads and greater normalized

displacements. Additionally, samples with machined inserts typically had more numerous and more pronounced examples of “kneeing” prior to net tension failure of the composite plate. However, the limited nature and variations within the results prevented further analysis. Digital Image correlation provided a method of comparing the types of inserts. In general, and consistent with previous research conducted on thick composites, stiffer insert, such as aluminum or steel performed best. These inserts showed smaller strain gradients across each cross section. Injected inserts, with the injection of the film adhesive, performed worst, sometimes resulting in strain gradients greater than the baseline tests.

Chapter 1, chapter 3, and chapter 4 assessed some of the advantages and disadvantages of using the injected inserts. The sealing aspect of injected inserts helped protect the connection from liquids or other particles. Injected inserts conformed to the geometry of the connection, lowering the tolerances when compared to a machine insert. Additionally, injected insert materials performed better in attenuating and distributing impulse forces. However, injected inserts consistently performed worse than machined inserts when subjected to static or simple tensile loads and the material removal from the bolt can substantially affect the failure mode of the bolted connection. In general, in applications where ultimate failure load is not the primary concern, injected inserts showed several advantages over a traditional machined insert.

Future Work

Several areas in which the injected insert research can be be furthered have been noted. The majority of research into inserts has been conducted in the static and quasi-static range; in this range it has been established stiffer inserts, typically aluminum or steel, will perform better than softer inserts, as used in injected inserts. However, in many instances, materials will

perform significantly differently under dynamic loading. A continuation of the research would be to perform similar experiments on the injected inserts in a single-lap shear joint using dynamic loading conditions.

The current research was conducted using a single-lap shear joint. Although a single-lap shear joint is simple to build and test, the configuration complicates the analysis of the samples. In addition to the tensile stress, the single-lap shear joint creates a bending moment on the sample which results in an uneven, and significantly more complicated, strain field across the sample. A continuation of the research would be to conduct experiments, such as simple tension of double-lap shear joints that eliminate the bending moment.

The current research was conducted using a limited number of commonly available injected insert materials. A continuation of the research would be to conduct experiments using a greater variety of commonly available materials as well as materials altered specifically for use in an injected insert, i.e. by using nano-particles or carbon fibers.

APPENDICES

APPENDIX A

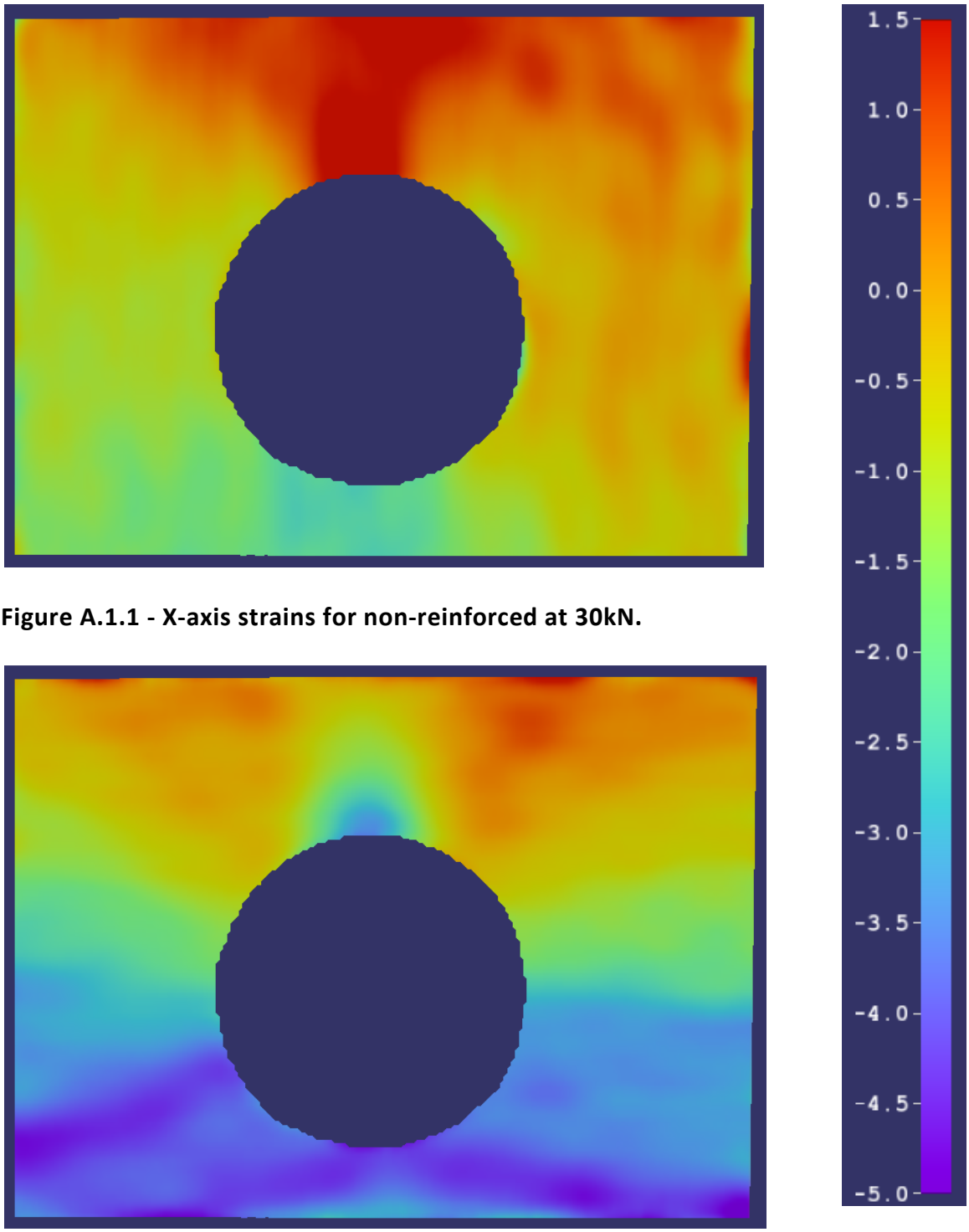

Figure A.1.1 - X-axis strains for non-reinforced at 30kN.

Figure A1.2 – Y-axis strains for non-reinforced at 30kN.

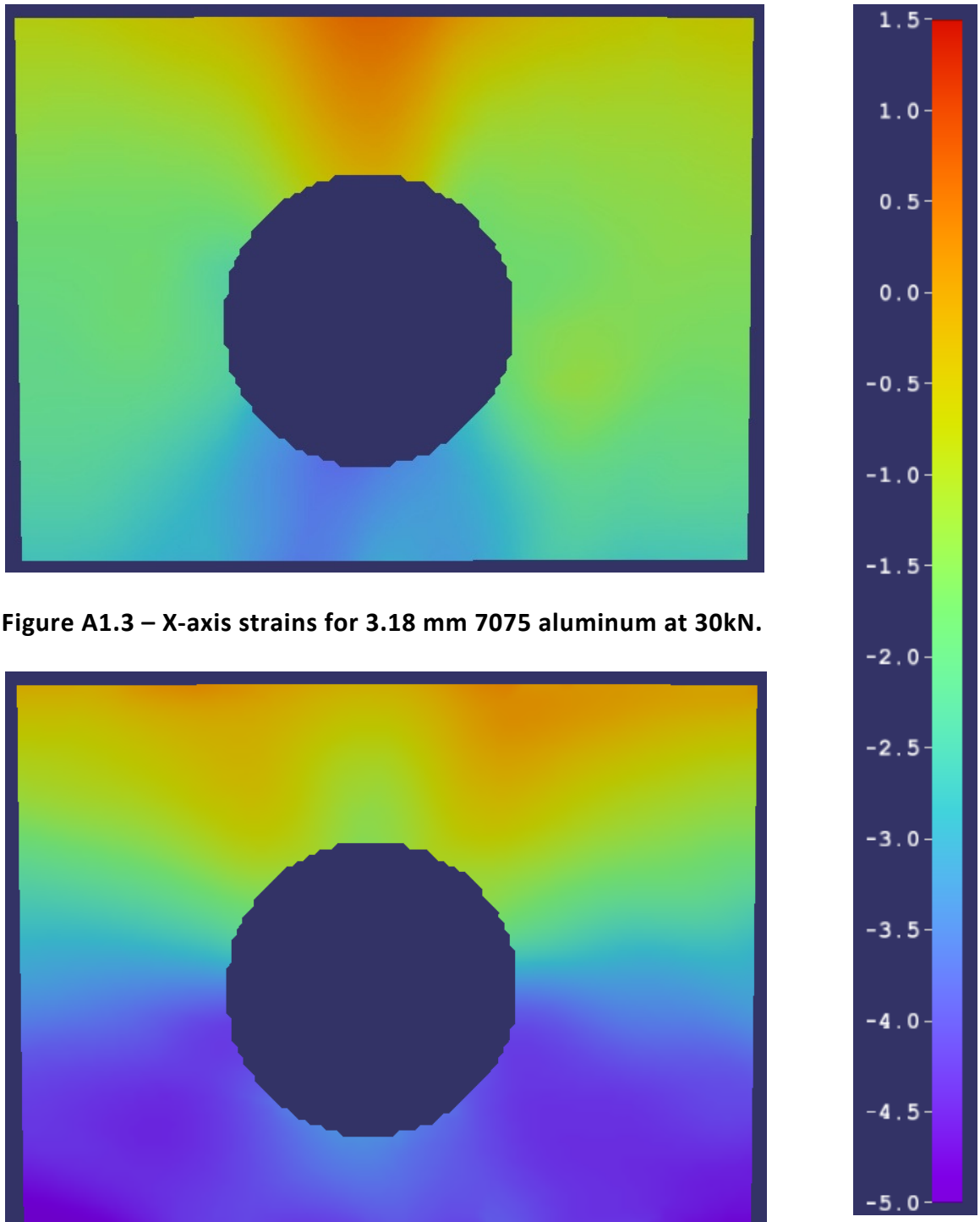

Figure A1.3 – X-axis strains for 3.18 mm 7075 aluminum at 30kN.

Figure A1.4 – Y-axis Strains for 3.18 mm 7075 aluminum at 30kN.

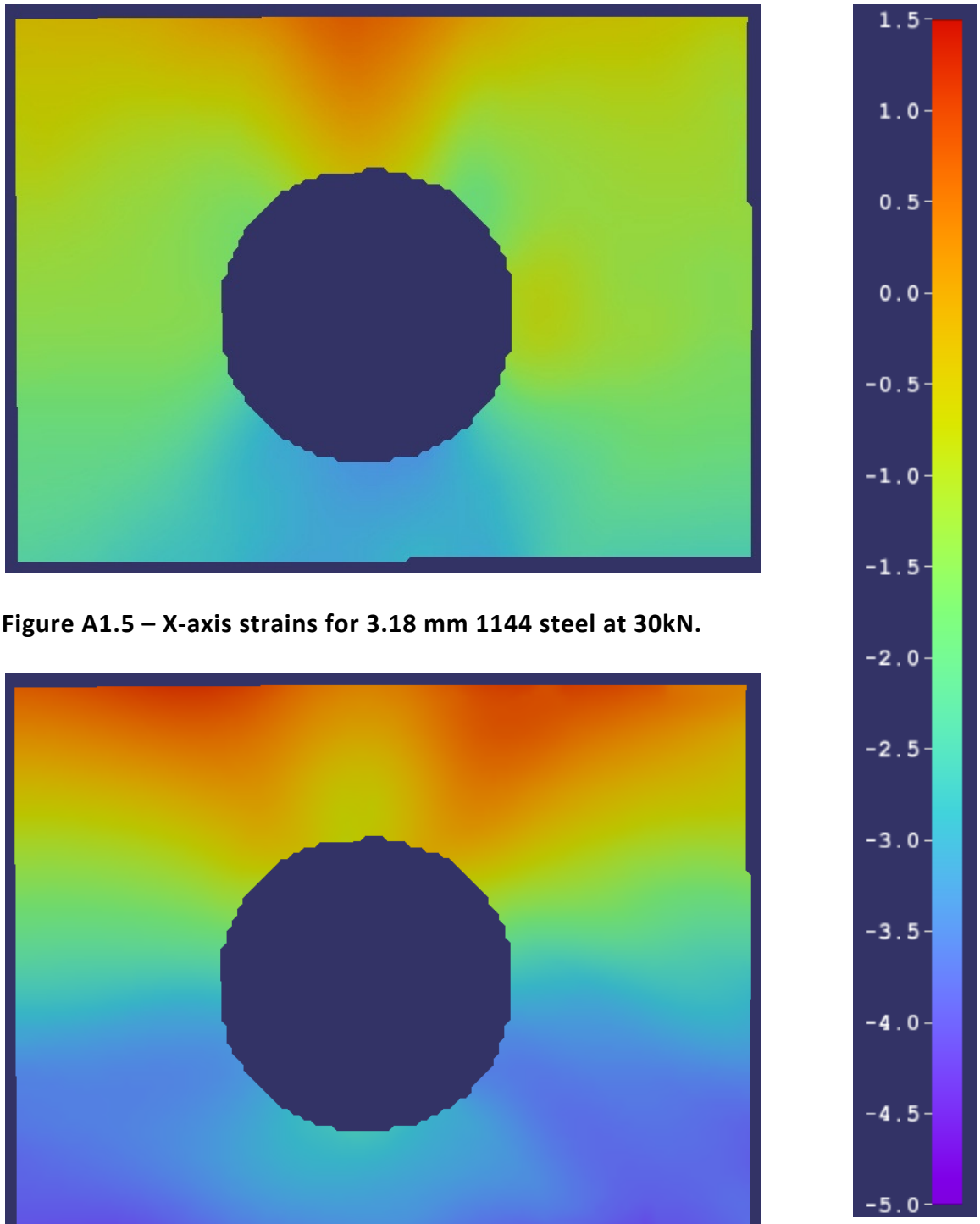

Figure A1.5 – X-axis strains for 3.18 mm 1144 steel at 30kN.

Figure A1.6 – Y-axis strains for 3.18 mm 1144 steel at 30kN.

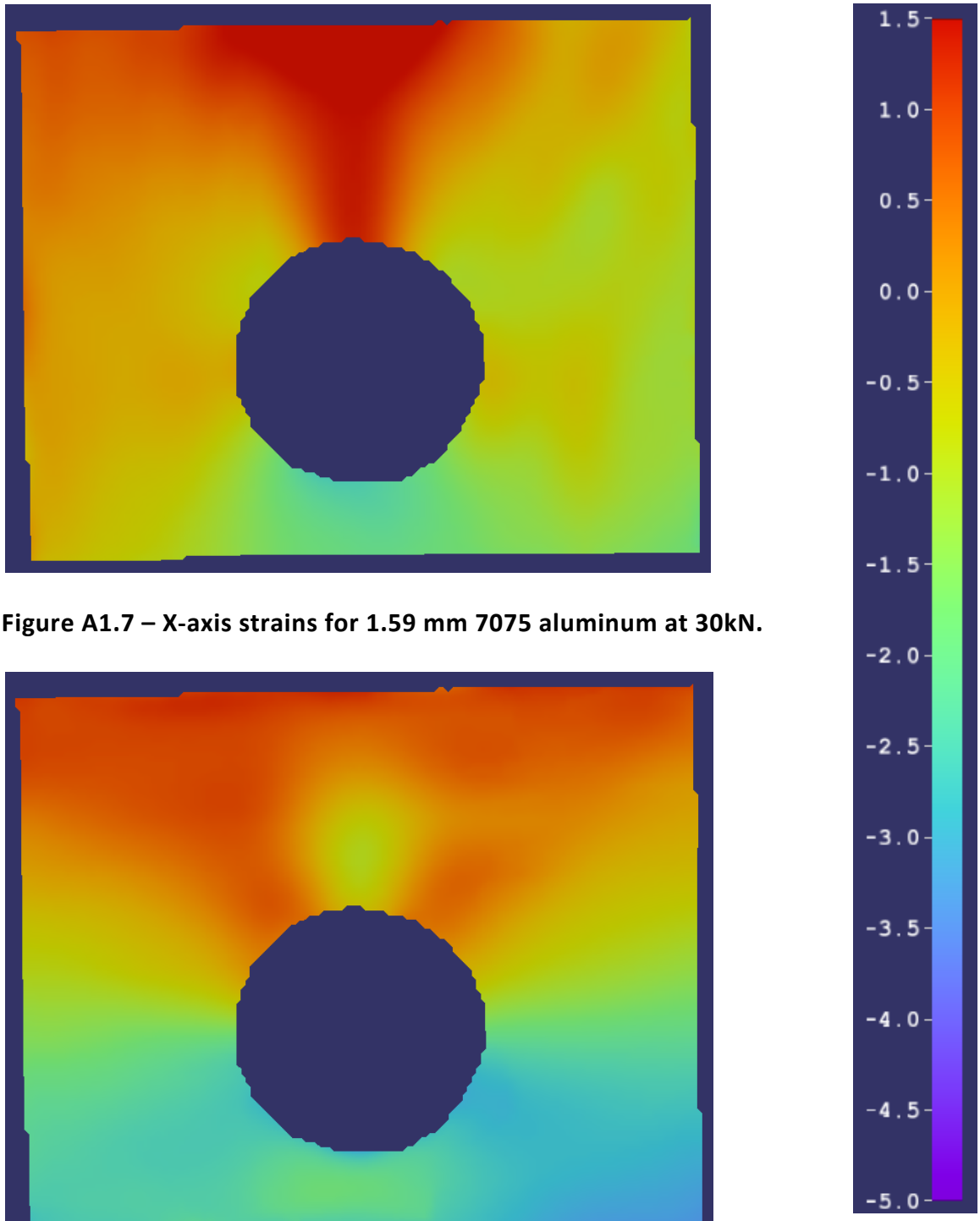

Figure A1.7 – X-axis strains for 1.59 mm 7075 aluminum at 30kN.

Figure A1.8 – Y-axis strains for 1.59 mm 7075 aluminum at 30kN.

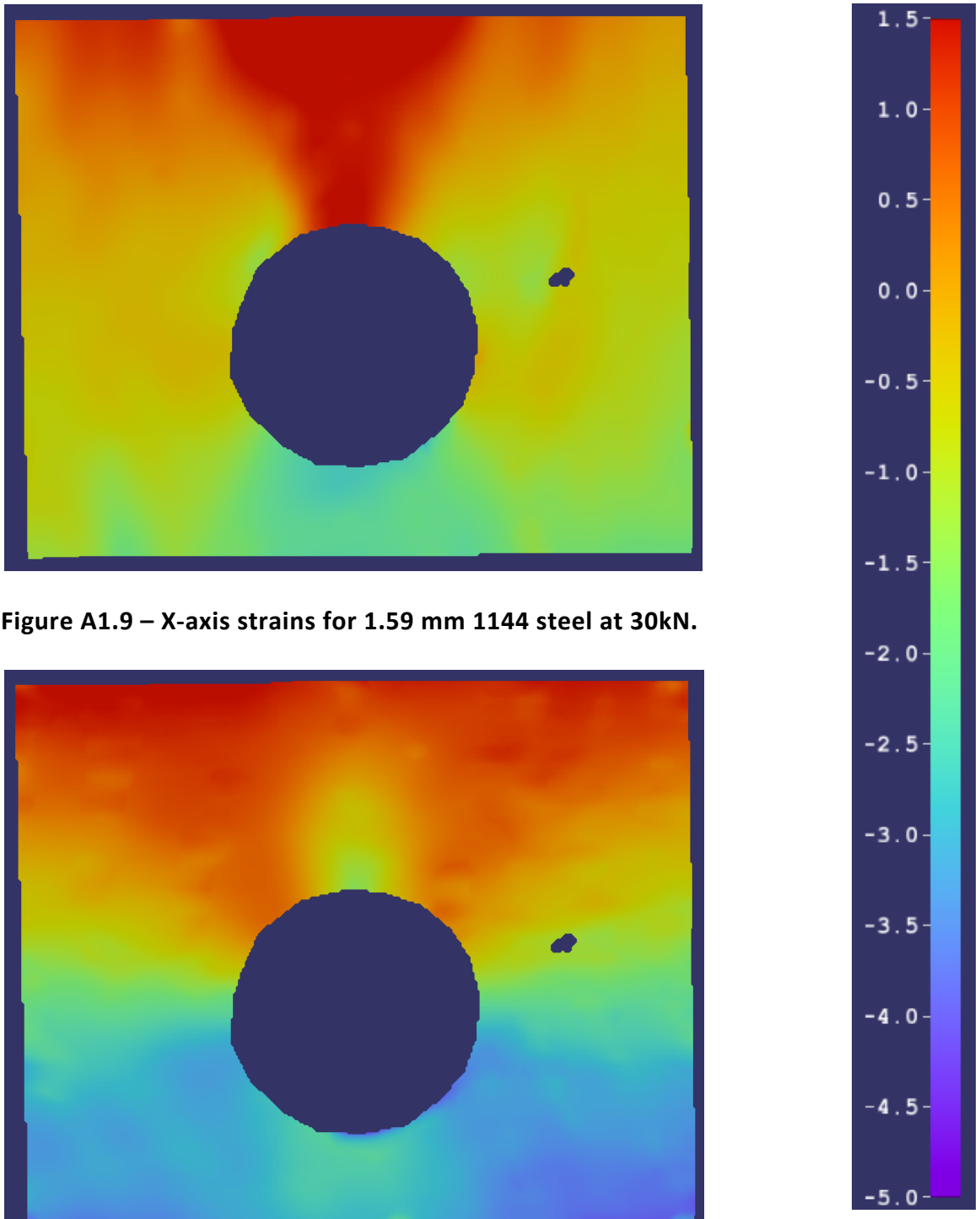

Figure A1.9 – X-axis strains for 1.59 mm 1144 steel at 30kN.

Figure A1.10 – Y-axis strains for 1.59 mm 1144 steel at 30kN.

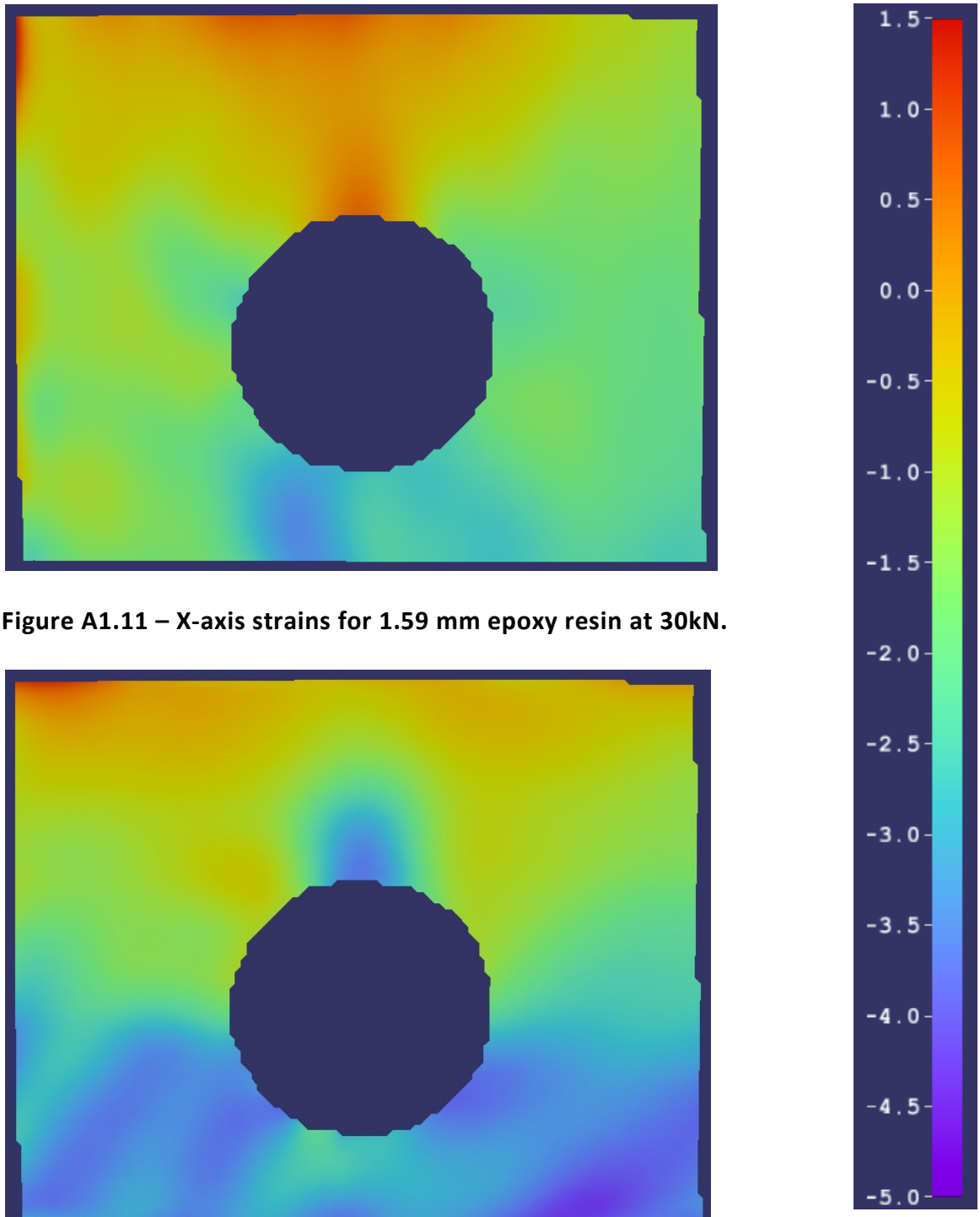

Figure A1.11 – X-axis strains for 1.59 mm epoxy resin at 30kN.

Figure A1.12 – Y-axis strains for 1.59 mm epoxy resin at 30kN.

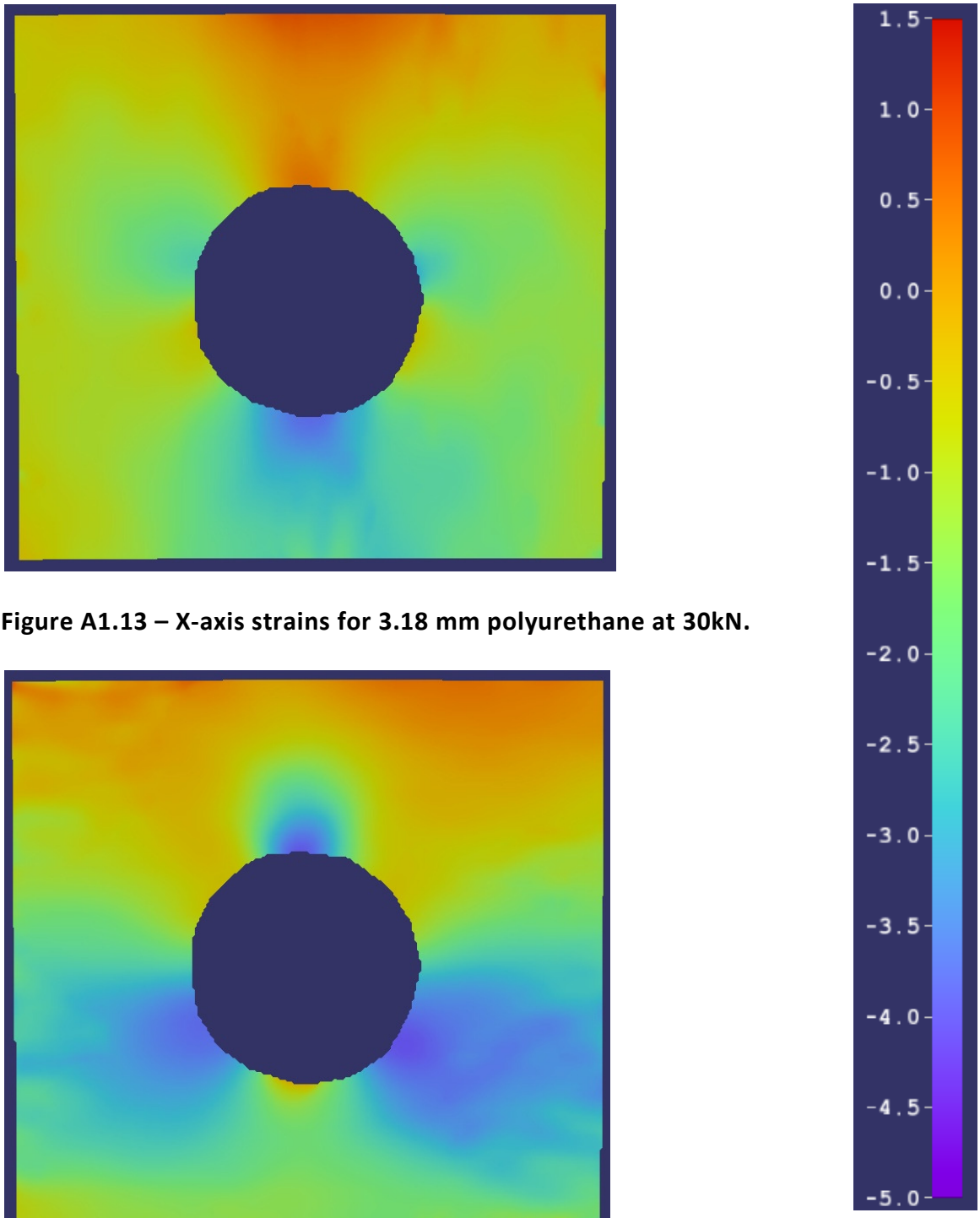

Figure A1.13 – X-axis strains for 3.18 mm polyurethane at 30kN.

Figure A1.14 – Y-axis strains for 1.59 mm polyurethane at 30kN.

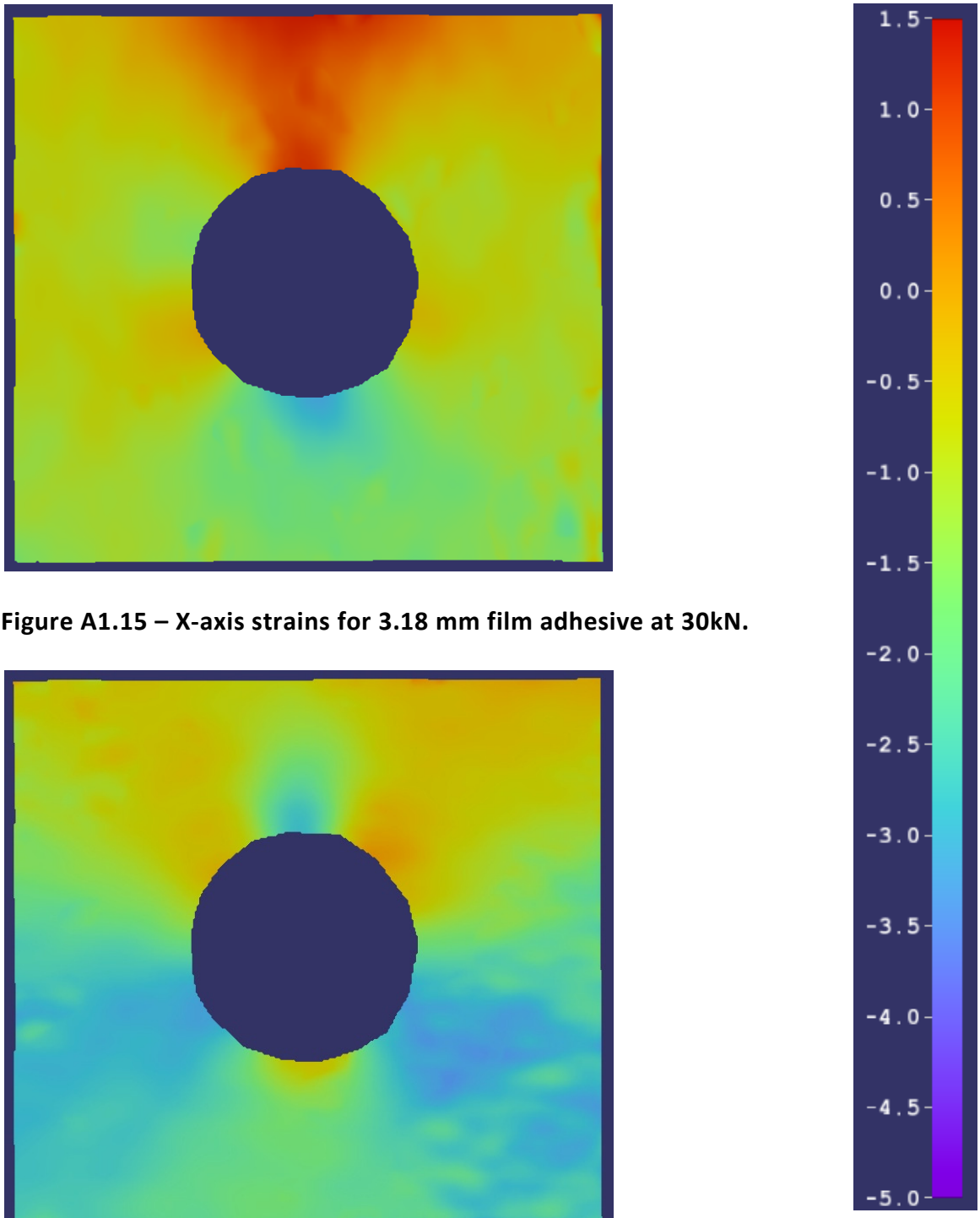

Figure A1.15 – X-axis strains for 3.18 mm film adhesive at 30kN.

Figure A1.16 – Y-axis strains for 1.59 mm film adhesive at 30kN.

REFERENCES

REFERENCES

[1] Nillsson, Sören. (1989) “Increasing Strength of Graphite/Epoxy Bolted Joints by Introducing an Adhesively Bonded Metallic Insert.” Journal of Composite Materials 23: 642-650

[2] Herrera-Franco, Pedro J., Cloud, Gary L. (1992) “Strain-Relief Inserts for Composite Fasteners –An Experimental Study.” Journal of Composite Materials 26: 751-768

[3] Camanho, P.P., Tavares, C.M.L., et al. (2005) “Increasing the efficiency of composite single-shear lap joints using bonded inserts.” Composites Part B: Engineering 36: 372-383

[4] Herrington, P.D., Sabbaghian, M. (1992) “Effect of Radial Clearance between Bolt and Washer on the Bearing Strength of Composite Bolted Joints.” Journal of Composite Materials 26: 1826-1843

[5] Riccio, A., Marciano, L. (2005) “Effects of Geometrical and Material Features on Damage Onset and Propagation in Single-Lap Bolted Composite Joints under Tensile Load: Part 1 – Experimental Studies.” Journal of Composite Materials 39: 2071-2090

[6] Eriksson, Ingvar. (1990) “On the Bearing Strength of Bolted Graphite/Epoxy Laminates.” Journal of Composite Materials 24: 1246-1269

[7] Ekh, Johan, Schon, Joakim, et al. (2005). “Secondary bending in multi fastener, composite-to-aluminum single shear lap joints.” Composites Part B 36:195-208

[8] McCarthy, M.A., McCarthy, C.T. et al. (2006). “A simple method for determining the effects of bolt-hole clearance on load distribution in single-column multi-bolt composite joints.” Composite Structures. 73:78-87

[9] Khashabam U.A., Sallam, H.E.M., et al. (2006) “Effect of washer size and tightening torque on the performance of bolted joints in composite structures.” Composite Structures. 73:310-317.

[10] Zaera, R., Sanchez, S., et al. (2000). “Modeling of the adhesive layer in mixed ceramic/metal armours subjected to impact. Composites Part A:. 31:823-833

[11] Lopez-Puente, J., Arias, A., et al. (2005) "The effect of the thickness of the adhesive layer on the ballistic limit of ceramic/metal amours. An experimental and numerical study." International Journal of Impact Engineering. 32:321-336.